

Energy-Efficient Designs for SIM-Based Broadcast MIMO Systems

Nemanja Stefan Perović, *Member, IEEE*, Eduard E. Bahingayi, *Member, IEEE*
and Le-Nam Tran, *Senior Member, IEEE*

Abstract—Stacked intelligent metasurface (SIM), which consists of multiple layers of intelligent metasurfaces, is emerging as a promising solution for future wireless communication systems. In this timely context, we focus on broadcast multiple-input multiple-output (MIMO) systems and aim to characterize their energy efficiency (EE) performance. To explore the potential of SIM, we consider both dirty paper coding (DPC) and linear precoding (LP) and formulate the corresponding EE maximization problems. For DPC, we employ the broadcast channel (BC)-multiple-access channel (MAC) duality to obtain an equivalent problem, and optimize users' covariance matrices using the successive convex approximation (SCA) and Dinkelbach's methods. Since the phase shift optimization problem of the SIM meta-elements is one of extremely large size, we adopt a conventional projected gradient-based method for its simplicity. A similar approach is followed for the case of LP. Simulation results show that the proposed optimization methods for the considered SIM-based systems can significantly improve the EE, compared to conventional counterparts. Also, we demonstrate that the number of SIM meta-elements and their distribution across the SIM layers have a significant impact on both the achievable sum-rate and EE performance.

Index Terms—Broadcast, energy efficiency (EE), multiple-input multiple-output (MIMO), optimization, stacked intelligent metasurface (SIM).

I. INTRODUCTION

The framework for the future development of International Mobile Telecommunications (IMT) for 2030 highlights sustainability as a fundamental goal for future communication systems, with the aim of minimizing environmental impact through efficient resource usage, reduced power consumption, and lower greenhouse gas emissions [1]. This has made energy-efficient wireless communications a key research focus. At the same time, global mobile network data traffic is projected to reach 563 exabytes (EBs) by 2029 [2], which requires the evolution of network technologies to meet the increasing demand. For example, conventional multiple-input

multiple-output (MIMO) systems are advancing toward massive MIMO (mMIMO) and ultra-massive MIMO (umMIMO) systems. However, these technologies face challenges in energy efficiency (EE) due to the substantial power consumption required to support a large number of radio frequency (RF) chains.

A promising solution to address these challenges is the use of reconfigurable intelligent surfaces (RISs), which consist of a large number of programmable metamaterial elements capable of dynamically tuning their electromagnetic (EM) properties. In this way, RISs can modify the incoming waves in a programmable and controllable manner [3]. This capability allows RISs to simultaneously improve multiple performance metrics, such as spectrum efficiency, EE, and coverage. Unfortunately, the significant path-loss of RIS-assisted links greatly limits the potential EE gains from RIS deployment.

To address the limitations of RIS, several innovative metamaterial-based antenna technologies such as holographic radio, dynamic metasurface antennas (DMAs), and stacked intelligent metasurfaces (SIMs) have been proposed. Holographic radio, also known as holographic MIMO (HMIMO), achieves high directive gain, spectral efficiency (SE) and EE by combining densely packing sub-wavelength metamaterial antenna elements with holographic techniques [4], [5]. Similarly, DMAs consist of multiple microstrips, each composed of a multitude of metamaterial radiating elements and connected to a single RF chain [6]. This design offers better EE than hybrid analog-to-digital (A/D) architectures by eliminating the need for additional power to support numerous phase shifters [7]. However, both HMIMOs and DMAs, as single-layer structures, often require a very large number of elements due to hardware constraints that limit the number of tunable amplitudes/phases.

In contrast, SIMs represent the latest advancement in metamaterial-based antenna technologies. Composed of multiple parallel metasurface layers with nearly passive, programmable meta-elements, SIMs can be integrated with conventional transceivers using a small number of active antennas, offering a low-cost and energy-efficient solution. Inspired by deep neural networks (DNN), SIMs perform signal processing tasks, such as transmit precoding and receive combining, directly in the EM domain when properly controlled and programmed [8]. The close spacing between active antennas and SIM layers significantly reduces the path-loss and eliminates the multiplicative path-loss effects seen in RIS-aided systems. By utilizing whole metasurfaces to achieve array gain and suppress co-channel interference in the EM wave

This work was supported by Taighde Éireann - Research Ireland under Grant 22/US/3847 and Grant 13/RC/2077_P2.

Nemanja Stefan Perović was with Université Paris-Saclay, CNRS, CentraleSupélec, Laboratoire des Signaux et Systèmes, 3 Rue Joliot-Curie, 91192 Gif-sur-Yvette, France. He is now with the Intelligent Wireless Communication (i-Wic) Laboratory, Institute of Communications Engineering, National Sun Yat-sen University, Kaohsiung 80424, Taiwan, R.O.C. (Email: n.s.perovic@mail.nsysu.edu.tw).

Eduard E. Bahingayi was with University College Dublin, Belfield, Dublin, Ireland. He is now with the Engineering Division, New York University Abu Dhabi (NYUAD), Abu Dhabi, UAE, 129188 (Email: eeb9783@nyu.edu).

Le-Nam Tran is with the School of Electrical and Electronic Engineering, University College Dublin, Belfield, Dublin 4, D04 V1W8, Ireland (Email: nam.tran@ucd.ie).

domain, SIMs reduce transmission power requirements while significantly enhancing EE and overall system performance, all with minimal hardware complexity.

Recent studies have investigated various applications of SIMs. In [9], SIMs were exploited to implement a 2D discrete Fourier transform (DFT) for direction of arrival (DOA) estimation. A hybrid channel estimator combining wave and digital domain processing was proposed in [10]. However, it requires perfect orthogonality between user pilot sequences, which is hard to achieve. In [11], the authors minimized the Cramer-Rao bound (CRB) for target estimation in an ISAC system with a SIM. Specifically, using an experimental SIM platform, they showed power variations across layers but without any physical explanation. A general path-loss model for SIM-assisted systems was developed in [12], based on which, algorithms aimed at maximizing the received power were derived. This design can generate complex radiation patterns but requires many layers for discrete phase shifts. Research on sum-rate maximization includes studies on SIM-assisted downlink MISO channels [13] and multi-user systems using statistical channel state information (CSI) [14]. In particular, it was shown that using statistical CSI yields slightly worse performance while achieving lower computational and processing overhead. In [15], deep reinforcement learning (DRL) was shown to outperform conventional optimization approaches for maximizing the sum rate in SIM-assisted communication systems. In uplink SIM-based cell-free MIMO systems, rate optimization using distributed signal processing was studied in [16]. In this scenario, each access point (AP) locally detects user information, which is then combined by the central processing unit (CPU) to recover the final data, though this process can demand substantial link resources in practice.

The integration of SIMs with transmitters and receivers into a SIM-based HMIMO system, capable of performing signal precoding and combining in the wave domain, was proposed in [17]. This system introduced a channel fitting approach that enables the SIM-based HMIMO system to achieve significant channel capacity gains compared to mMIMO and RIS-assisted counterparts. An approach for the mutual information maximization in a SIM-based HMIMO system with discrete signaling was presented in [18], using the cutoff rate as an alternative metric. This study demonstrates that incorporating even a small-scale digital precoder into the system can substantially increase its mutual information.

Despite extensive research on SIM-assisted systems, the EE analysis of SIM-assisted MIMO systems remains largely unexplored. Notably, EE optimization inherently includes SE maximization and transmit power minimization as special cases. Motivated by this gap, we aim to maximize the EE in SIM-aided broadcast systems using dirty paper coding (DPC) and linear precoding (LP). To solve the formulated EE maximization (EEmax) problems, we blend multiple optimization techniques to derive efficient problem-driven algorithms, leveraging the special structure of the considered problems and suitable optimization tools. For DPC, we formulate a joint optimization problem of the covariance matrix of the transmitted signal and the phase shifts of the SIM meta-elements. In the more practical case of LP, we consider a

similar joint optimization problem for transmit precoding and SIM phase shifts. For both scenarios, we assume a limited total power budget and impose unit modulus constraints on the SIM meta-elements. Furthermore, perfect CSI is assumed at the BS to explore the full EE potential of SIM-based systems. Note that we do not optimize the number of active transmit antennas, which is left for future work. The main contributions of this paper are summarized as follows:

- For DPC, we exploit the well-known Gaussian MIMO broadcast channel (BC)-multiple-access channel (MAC) duality to reformulate the EEmax problem in terms of users' covariance matrices in the MAC and the phase shifts of the SIM meta-elements. Within the adopted alternating optimization (AO) framework, we present an efficient solution for optimizing the covariance matrices, using a tight concave lower bound of the achievable sum-rate via the successive convex approximation (SCA) method. Dinkelbach's method is then applied to obtain closed-form expressions for the optimal covariance matrices. Our complexity analysis demonstrates that our proposed method has significantly lower complexity compared to an existing solution [19]. For optimizing the SIM phase shifts, we employ a projected gradient-based method to update all SIM layers in parallel. This approach is viable considering the large size of the considered problem. In this context, we derive closed-form expressions for the complex-valued gradients involved.
- For LP, we leverage a recent result for the sum-rate maximization that allows for reformulating the considered EEmax problem as an equivalent one, with a greatly reduced dimension. Following this important step, we again invoke the SCA method to derive a quadratic lower bound of the achievable sum-rate and approximate the EEmax problem as a concave fractional program. Next, we apply Dinkelbach's method to solve the resulting problem, obtaining optimal users' precoders in closed-form expressions. Similar to the DPC-based scheme, the phase shifts of the SIM meta-elements in this setting are optimized in parallel using a conventional projected gradient-based method.
- We present efficient implementations of the proposed algorithms, analyze their computational complexity in terms of the number of complex multiplications, and mathematically prove their convergence.
- We show through simulation results that the proposed algorithms substantially increase the EE in SIM-aided broadcast communication systems, with greater improvements observed for DPC. The results highlight the importance of the proposed precoding schemes in mitigating multi-user interference, especially in systems with a large number of users. We also provide several valuable insights into the design and performance of energy-efficient SIM-based broadcast MIMO systems. First, the EE increases logarithmically with the number of meta-elements per SIM layer, with a nearly double gain when increasing from 49 to 100 compared to 100 to 196. Second, SIM-aided systems with a low number of meta-elements may

TABLE I
NOTATION DESCRIPTION.

Symbol	Description
\mathbf{H}	Matrix
\mathbf{h}	Row/column vector
$\mathbb{C}^{m \times n}$	Space of $m \times n$ complex matrices
\mathbf{H}^T	Transpose of \mathbf{H}
\mathbf{H}^H	Hermitian transpose of \mathbf{H}
$ \mathbf{H} $	Determinant of \mathbf{H}
$\text{Tr}(\mathbf{H})$	Trace of \mathbf{H}
$\log_2(\cdot)$	Binary logarithm
$\ln(\cdot)$	Natural logarithm
$(\cdot)^+$	Pseudo-inverse operation
$\lfloor \cdot \rfloor$	Floor operation
$(\cdot)^*$	Complex conjugate
$\ \mathbf{H}\ $	Frobenius norm
$\text{vec}_d(\mathbf{H})$	Vector consisting of the diagonal elements of \mathbf{H}
$\mathbf{A} \succeq (\succ) \mathbf{B}$	$\mathbf{A} - \mathbf{B}$ is positive semidefinite (definite)
\mathbf{I}	Identity matrix
$\Re(\mathbf{x})$	Real part of \mathbf{x}
$\Im(\mathbf{x})$	Imaginary part of \mathbf{x}
$\text{diag}(\mathbf{x})$	Matrix with the elements of \mathbf{x} on the main diagonal
$\mathcal{CN}(\cdot, \cdot)$	Circularly symmetric complex Gaussian distribution
$ x $	Modulus of the number x
$ \mathbf{H} $	Determinant of \mathbf{H}
$\nabla_{\mathbf{x}} f(\cdot)$	Complex gradient of $f(\cdot)$ with respect to (w.r.t.) \mathbf{x}^*

have lower EE than conventional MIMO systems without SIM integration. Third, a few SIM layers suffice to balance SE gains and power consumption for optimal EE. Fourth, in SIM-aided broadcast systems *without digital precoding*, optimal EE is achieved by activating a subset of transmit antennas, each transmitting independent data streams. Lastly, at least 3 bits per meta-element are required to keep EE degradation from quantization errors within acceptable limits.

The mathematical notation used in this paper is summarized in Table I.

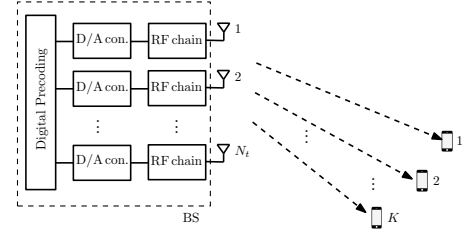
II. SYSTEM MODEL AND PROBLEM FORMULATION

A. System Model

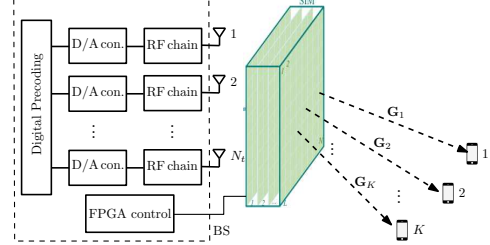
System level diagrams of conventional and SIM-aided broadcast systems are shown in Fig. 1. In both cases, we consider a multi-user broadcast system in which a BS with N_t transmit antennas communicates with K users, each equipped N_r receive antennas. The main difference is in the presence of a SIM at the BS, which comprises of L metasurface layers, each containing N meta-elements. The SIM is controlled by external field programmable gate array (FPGA) devices, which adjust the phase shifts of individual meta-elements for wave domain beamforming.¹ For the sake of simplicity, we assume that this device is integrated into the BS hardware and communicates with the SIM via a dedicated interface.

The phase shifts of the meta-elements in the l -th SIM layer are represented by the diagonal matrix $\Phi^l = \text{diag}(\phi^l) = \text{diag}([\phi_1^l \ \phi_2^l \ \dots \ \phi_N^l]^T)$, where $\phi_n^l = \exp(j\theta_n^l)$ and θ_n^l is the phase shift of the n -th element in the l -th layer. Signal propagation between two consecutive layers, $l-1$ and l , is modeled by the matrix $\mathbf{W}^l \in \mathbb{C}^{N \times N}$ for $l = 2, 3, \dots, L$.

¹By considering both SIM (i.e., wave-based precoding) and digital precoding, our system model is general enough to include the wave-based only precoding and digital only precoding as special cases.



(a) Conventional broadcast system.



(b) SIM-aided broadcast system.

Fig. 1. System level diagrams of conventional and SIM-aided broadcast systems.

Specifically, the signal propagation between the n -th meta-element of the $(l-1)$ -th and the m -th meta-element of l -th layer of the SIM is presented by [20, Eq. (1)]

$$[\mathbf{W}^l]_{m,n} = \frac{A_k \cos \chi_{m,n}}{d_{m,n}} \left(\frac{1}{2\pi d_{m,n}} - \frac{j}{\lambda} \right) e^{j \frac{2\pi d_{m,n}}{\lambda}} \quad (1)$$

where A_k is the area of each meta-element, $d_{m,n}$ is the distance between the meta-elements of these two layers, $\chi_{m,n}$ is the angle between the propagation direction and the normal to the $(l-1)$ -th layer, and λ is the wavelength. The signal propagation between the transmit antenna array and the first layer of the SIM is represented by the matrix $\mathbf{W}^1 \in \mathbb{C}^{N \times N_t}$, whose elements can be calculated as in (1).

The end-to-end channel matrix between the BS and the k -th user is expressed as

$$\mathbf{H}_k = \mathbf{G}_k \mathbf{B} \in \mathbb{C}^{N_r \times N_t} \quad (2)$$

where $\mathbf{G}_k \in \mathbb{C}^{N_r \times N}$ denotes the channel matrix between the final layer of the SIM and user k , and $\mathbf{B} = \Phi^L \mathbf{W}^L \dots \Phi^2 \mathbf{W}^2 \Phi^1 \mathbf{W}^1 \in \mathbb{C}^{N \times N_t}$ is the EM response of the transmit SIM. We assume that \mathbf{G}_k is perfectly known to the BS to investigate its full theoretical potential.

B. Dirty Paper Coding (DPC)

To evaluate an upper bound on achievable EE, we first consider DPC, which achieves the capacity region of a Gaussian MIMO BC. The received signal at user k is given by

$$\mathbf{y}_k = \mathbf{H}_k \mathbf{s}_k + \sum_{j < k} \mathbf{H}_k \mathbf{s}_j + \sum_{j > k} \mathbf{H}_k \mathbf{s}_j + \mathbf{n}_k \quad (3)$$

where $\mathbf{H}_k \in \mathbb{C}^{N_r \times N_t}$ is the channel matrix for user k , $\mathbf{s}_k \in \mathbb{C}^{N_t \times 1}$ is the transmitted signal for user k . The noise vector $\mathbf{n}_k \in \mathbb{C}^{N_r \times 1}$ consists of independent and identically distributed (i.i.d.) elements that are distributed according to $\mathcal{CN}(0, \sigma^2)$, where σ^2 is the noise variance.

The BS designs \mathbf{s}_k with full (non-causal) knowledge of the interference term $\sum_{j < k} \mathbf{H}_k \mathbf{s}_j$, which results from transmissions to users $1, 2, \dots, k-1$. Therefore, DPC can eliminate

this interference from previously encoded users, and thus, only the interference caused by users $k+1, \dots, K$ remains. Based on this, the achievable rate of user k is given by

$$R_{\text{BC},k}(\mathbf{Q}, \phi) = \ln \frac{\left| \mathbf{I} + \mathbf{H}_k (\sum_{j \geq k} \mathbf{Q}_j) \mathbf{H}_k^H \right|}{\left| \mathbf{I} + \mathbf{H}_k (\sum_{j > k} \mathbf{Q}_j) \mathbf{H}_k^H \right|}, \quad (4)$$

where, by slight abuse of notation, \mathbf{H}_k stands for \mathbf{H}_k/σ (i.e., \mathbf{H}_k is normalized by the square root of the noise power), $\mathbf{Q}_k = \mathbb{E}\{\mathbf{s}_k \mathbf{s}_k^H\} \succeq \mathbf{0}$ is the input covariance matrix of user k , $\mathbf{Q} = [\mathbf{Q}_1, \mathbf{Q}_2, \dots, \mathbf{Q}_K]$ and $\phi = [(\phi^1)^T, (\phi^2)^T, \dots, (\phi^L)^T]^T$. These covariance matrices are constrained by the total power budget as

$$\sum_{k=1}^K \text{Tr}(\mathbf{Q}_k) \leq P_{\text{max}} \quad (5)$$

where P_{max} is the available transmit power budget.

C. Multi-user MIMO with LP

Although DPC is a capacity achieving scheme, it has high complexity due to its nonlinear coding nature. On the other hand, LP is much simpler to implement in practice. For LP, the transmitted signal is expressed as

$$\mathbf{x} = \sum_{k=1}^K \mathbf{P}_k \mathbf{s}_k \quad (6)$$

where \mathbf{s}_k is the signal intended for user k and $\mathbf{P}_k \in \mathbb{C}^{N_t \times N_r}$ is the corresponding linear precoder. Thus, the received signal at user k is given by

$$\mathbf{y}_k = \mathbf{H}_k \mathbf{x} + \mathbf{n}_k = \mathbf{H}_k \mathbf{P}_k \mathbf{s}_k + \sum_{j=1, j \neq k}^K \mathbf{H}_k \mathbf{P}_j \mathbf{s}_j + \mathbf{n}_k. \quad (7)$$

By treating the multiuser interference as Gaussian noise, the achievable rate of user k is given by

$$R_{\text{L},k}(\mathbf{P}, \phi) = \ln \left| \mathbf{I} + \mathbf{H}_k \mathbf{P}_k \mathbf{P}_k^H \mathbf{H}_k^H \right. \\ \left. \times \left(\mathbf{I} + \sum_{j=1, j \neq k}^K \mathbf{H}_k \mathbf{P}_j \mathbf{P}_j^H \mathbf{H}_k^H \right)^{-1} \right| \quad (8)$$

where $\mathbf{H}_k = \mathbf{H}_k/\sigma$ and the precoding matrices $\mathbf{P} = [\mathbf{P}_1, \mathbf{P}_2, \dots, \mathbf{P}_K]$ have to satisfy the total power constraint:

$$\sum_{k=1}^K \text{Tr}(\mathbf{P}_k \mathbf{P}_k^H) \leq P_{\text{max}}. \quad (9)$$

Note that the achievable rate of user k can alternatively be expressed using covariance matrices by defining $\mathbf{Q}'_k = \mathbf{P}_k \mathbf{P}_k^H$. However, \mathbf{Q}'_k differs from \mathbf{Q}_k for DPC because of differences in the rate expressions. Some existing solutions impose $\text{rank}(\mathbf{Q}_k) = N_r$ to derive \mathbf{P}_k , but we do not adopt this approach because optimizing $\{\mathbf{Q}'_k\}$ introduces additional computational complexity compared to directly optimizing $\{\mathbf{P}_k\}$.

D. Problem Formulation

The objective is to maximize the EE of the considered communication system, which is defined as the ratio of the sum-rate and the total power consumption. The total power

consumption is modeled as $P_{\text{tot}} = P_t + N_t P_c + P_0 + L N P_s$, where

$$P_t = \begin{cases} \sum_{k=1}^K \text{Tr}(\mathbf{Q}_k) & \text{DPC} \\ \sum_{k=1}^K \text{Tr}(\mathbf{P}_k \mathbf{P}_k^H) & \text{LP} \end{cases} \quad (10)$$

is the data-dependent transmit signal power, P_c is the circuit power per RF chain (including the appropriate DVA converter), P_0 is the standby power consumed at the BS, and P_s is the power consumption of the switching circuits (e.g., PIN diodes, varactor diodes) of each SIM meta-element.² Since BSs dominate power consumption in mobile networks, user power consumption is excluded from the EE optimization in this study.

For the DPC-based scheme, the EE maximization (EEmax) problem is stated as

$$\max_{\mathbf{Q}, \phi} \eta_{\text{DPC}} = \frac{W \sum_{k=1}^K R_{\text{BC},k}(\mathbf{Q}, \phi)}{\sum_{k=1}^K \text{Tr}(\mathbf{Q}_k) + N_t P_c + P_0 + L N P_s} \quad (11a)$$

$$\text{s.t. } |\phi_n^l| = 1, \forall l, n \quad (11b)$$

$$\sum_{k=1}^K \text{Tr}(\mathbf{Q}_k) \leq P_{\text{max}}; \mathbf{Q}_k \succeq \mathbf{0}, \forall k, \quad (11c)$$

where W is the system bandwidth. Similarly, the EEmax problem with LP is written as

$$\max_{\mathbf{P}, \phi} \eta_{\text{LP}} = \frac{W \sum_{k=1}^K R_{\text{L},k}(\mathbf{P}, \phi)}{\sum_{k=1}^K \text{Tr}(\mathbf{P}_k \mathbf{P}_k^H) + N_t P_c + P_0 + L N P_s} \quad (12a)$$

$$\text{s.t. } |\phi_n^l| = 1, \forall l, n \quad (12b)$$

$$\sum_{k=1}^K \text{Tr}(\mathbf{P}_k \mathbf{P}_k^H) \leq P_{\text{max}}. \quad (12c)$$

Note that the equality constraints in (11b) and (12b) are treated element-wise. Since W is constant, it is dropped when solving (11) and (12), but included in simulation results in Section VII. Next, we present our proposed methods for solving the above two EEmax problems.

III. PROPOSED SOLUTION TO DPC-BASED SIM

To solve (11), we present an iterative optimization algorithm that alternates between optimizing the covariance matrices and the SIM phase shifts, a prevailing method in SIM-related studies. In particular, for fixed phase shifts, we propose a novel method to optimize the covariance matrices in parallel, using a closed-form water-filling solution, which allocates more transmit power to “stronger” user channels. This nice result is achieved by applying Dinkelbach’s method to iteratively maximize a quadratic lower bound of the objective function. The phase shifts of the SIM meta-elements are optimized by a gradient-based optimization method, which is a viable choice, considering the extremely large size of the SIM.

A. Covariance Matrix Optimization

For ease of readability, we briefly outlined the steps for optimizing covariance matrices as follows:

- Reformulate (11) using the BCs-MACs duality to obtain a more tractable equivalent formulation.

²In this model, we assume that the FPGA control and driving circuits of the SIM are integrated into the BS hardware, and the power consumption of these circuits is already included in the BS power consumption, P_0 .

- Derive a quadratic lower bound for the achievable sum-rate under the SCA framework.
- Apply Dinkelbach's method to solve the fractional EE objective, leading to a water-filling solution for the covariance matrices.

1) *Problem Reformulation:* The EEmax problem in (11a) is challenging to solve since its objective function is neither convex nor concave with respect to the optimization variables. To deal with this, we exploit the well-known duality between BCs and MACs [21], which states that the capacity region of the MIMO BC is equal to the capacity achieving region of the dual MIMO MAC. For single-user MIMO systems, this duality means that the capacity of a downlink channel \mathbf{H} equals that of a dual uplink channel \mathbf{H}^H under the same power constraint, which is easily understood. Extending this idea to multi-user MIMO systems, for a given channel between the BS and user k , the BC channel \mathbf{H}_k corresponds to the dual MAC channel \mathbf{H}_k^H . Similarly, each transmit covariance matrix \mathbf{Q}_k in the BC has as its counterpart a corresponding dual covariance matrix \mathbf{S}_k in the dual MAC.³ Accordingly, (11) is equivalent to the EEmax problem in the dual MAC, which is expressed as

$$\underset{\mathbf{S}}{\text{maximize}} \quad \frac{\ln \left| \mathbf{I} + \sum_{k=1}^K \mathbf{H}_k^H \mathbf{S}_k \mathbf{H}_k \right|}{\sum_{k=1}^K \text{Tr}(\mathbf{S}_k) + N_t P_c + P_0 + LNP_s} \quad (13a)$$

$$\sum_{k=1}^K \text{Tr}(\mathbf{S}_k) \leq P_{\max}; \mathbf{S}_k \succeq \mathbf{0}, \forall k, \quad (13b)$$

where we have omitted (11b) as the phase shifts are fixed, and the power constraint (13b) has the same maximum power as (11c). To solve (13) efficiently, we *temporarily* drop the power constraint (11c), which results in

$$\underset{\mathbf{S}_{k \geq 0}}{\text{maximize}} \quad g(\mathbf{S}) = \frac{\ln \left| \mathbf{I} + \sum_{k=1}^K \mathbf{H}_k^H \mathbf{S}_k \mathbf{H}_k \right|}{\sum_{k=1}^K \text{Tr}(\mathbf{S}_k) + N_t P_c + P_0 + LNP_s}. \quad (14)$$

To appreciate the novelty of our proposed method, we briefly describe the block-coordinate method proposed in [19], which optimizes each \mathbf{S}_k sequentially, while other variables are fixed. More precisely, let $\mathbf{S}^{(n)} = [\mathbf{S}_1^{(n)}, \mathbf{S}_2^{(n)}, \dots, \mathbf{S}_K^{(n)}]$ denote the current iterate. Then the next iterate $\mathbf{S}_k^{(n+1)}$ is obtained as

$$\begin{aligned} \mathbf{S}_k^{(n+1)} &= \arg \max_{\mathbf{S}_k \succeq \mathbf{0}} g(\mathbf{S}_1^{(n+1)}, \dots, \mathbf{S}_{k-1}^{(n+1)}, \mathbf{S}_k, \mathbf{S}_{k+1}^{(n)}, \dots, \mathbf{S}_K^{(n)}) \\ &= \arg \max_{\mathbf{S}_k \succeq \mathbf{0}} \frac{\ln |\mathbf{Z}_k| + \ln \left| \mathbf{I} + \mathbf{T}_k^H \mathbf{S}_k \mathbf{T}_k \right|}{p_k + \text{Tr}(\mathbf{S}_k)} \end{aligned} \quad (15)$$

where $\mathbf{Z}_k = \mathbf{I} + \sum_{j=1, j \neq k}^K \mathbf{H}_j^H \mathbf{S}_j \mathbf{H}_j$, $\mathbf{T}_k = \mathbf{H}_k \mathbf{Z}_k^{-1/2}$, and $p_k = \sum_{j=1, j \neq k}^K \text{Tr}(\mathbf{S}_j) + N_t P_c + P_0 + LNP_s$. Next, to solve (15), the authors of [19] applied Dinkelbach's method, which leads to the following problem

$$\max_{\mathbf{S}_k \succeq \mathbf{0}} F_\lambda(\mathbf{S}) \triangleq \ln |\mathbf{Z}_k| + \ln \left| \mathbf{I} + \mathbf{T}_k^H \mathbf{S}_k \mathbf{T}_k \right| - \lambda_D (p_k + \text{Tr}(\mathbf{S}_k)) \quad (16)$$

where λ_D is a non-negative parameter. For a given λ_D , the above problem can be solved in closed-form [19]. However, such a method requires finding the inverse of $\mathbf{Z}_k \in \mathcal{C}^{N_t \times N_t}$

³It should be noted that \mathbf{Q}_k can not be directly mapped to \mathbf{S}_k . Instead, it is required to compute first $\mathbf{S}_K, \mathbf{S}_{K-1}, \dots, \mathbf{S}_{k+1}$ before obtaining \mathbf{S}_k [21].

which has a complexity of $\mathcal{O}(N_t^3)$ in general, and computing the singular value decomposition (SVD) of \mathbf{T}_k which has a complexity of $\mathcal{O}(N_t^2 N_r)$. Thus, the overall complexity of the method presented in [19] is very high.

2) *SCA Method: A Tight Lower Bound of Sum Rate:* We now propose a more efficient method by leveraging the fact that a stationary solution to (14) is also globally optimal since (14) is a *concave-convex program*. This observation motivates us to adopt the SCA framework, which is typically used to find a stationary solution for nonconvex programs. To proceed, since $\mathbf{S}_k \succeq \mathbf{0}$, we can write $\mathbf{S}_k = \mathbf{U}_k^H \mathbf{U}_k$ where $\mathbf{U}_k \in \mathcal{C}^{N_r \times N_r}$. Thus, (14) is equivalent to the following unconstrained optimization problem:

$$\underset{\mathbf{U}_k}{\text{maximize}} \quad g(\mathbf{U}) = \frac{h(\mathbf{U})}{\sum_{k=1}^K \text{Tr}(\mathbf{U}_k^H \mathbf{U}_k) + N_t P_c + P_0 + LNP_s}. \quad (17)$$

where $h(\mathbf{U}) = \ln \left| \mathbf{I} + \sum_{k=1}^K \mathbf{H}_k^H \mathbf{U}_k^H \mathbf{U}_k \mathbf{H}_k \right|$ and $\mathbf{U} = [\mathbf{U}_1, \mathbf{U}_2, \dots, \mathbf{U}_K]$. It is easy to see that $h(\mathbf{U})$ can be equivalently rewritten as

$$\begin{aligned} h(\mathbf{U}) &= \sum_{j=1}^K \ln \left| \mathbf{I} + \left(\mathbf{I} + \sum_{k=j+1}^K \mathbf{H}_k^H \mathbf{U}_k^H \mathbf{U}_k \mathbf{H}_k \right)^{-1} \mathbf{H}_j^H \mathbf{U}_j^H \mathbf{U}_j \mathbf{H}_j \right| \\ &= \sum_{j=1}^K \ln \left| \mathbf{I} + \mathbf{U}_j \mathbf{H}_j \left(\mathbf{I} + \sum_{k=j+1}^K \mathbf{H}_k^H \mathbf{U}_k^H \mathbf{U}_k \mathbf{H}_k \right)^{-1} \mathbf{H}_j^H \mathbf{U}_j^H \right|. \end{aligned}$$

In fact, the j -th term in the sum above is the capacity of user j in the dual MAC, using successive interference cancellation [21]. As shown shortly, the above reformulation of $h(\mathbf{U})$ allows for approximating $h(\mathbf{U})$ by a "proper bound" to obtain a subproblem that admits a closed-form solution. In this regard, we recall the following inequality [22]:

$$\begin{aligned} \ln \left| \mathbf{I} + \mathbf{V} \mathbf{V}^{-1} \mathbf{V}^H \right| &\geq \ln \left| \mathbf{I} + \hat{\mathbf{V}} \hat{\mathbf{Y}}^{-1} \hat{\mathbf{V}}^H \right| - \text{Tr}(\hat{\mathbf{V}} \hat{\mathbf{Y}}^{-1} \hat{\mathbf{V}}^H) \\ &\quad + 2\Re(\text{Tr}(\hat{\mathbf{V}} \hat{\mathbf{Y}}^{-1} \mathbf{V}^H)) - \text{Tr}(\mathbf{A}^H (\mathbf{V}^H \mathbf{V} + \mathbf{Y})), \end{aligned} \quad (19)$$

where $\mathbf{A} = \hat{\mathbf{Y}}^{-1} - (\hat{\mathbf{V}}^H \hat{\mathbf{V}} + \hat{\mathbf{Y}})^{-1}$. We remark that the above inequality holds for arbitrary \mathbf{V} , $\hat{\mathbf{V}}$, $\mathbf{Y} \succ \mathbf{0}$ and $\hat{\mathbf{Y}} \succ \mathbf{0}$, provided that their sizes are compatible and the equality occurs when $\mathbf{V} = \hat{\mathbf{V}}$ and $\mathbf{Y} = \hat{\mathbf{Y}}$. In light of the SCA framework, we denote by $\mathbf{U}_j^{(n)}$ the value of \mathbf{U}_j after n iterations. Let

$$\mathbf{V} = \mathbf{U}_j \mathbf{H}_j \triangleq \mathbf{V}_j \in \mathcal{C}^{N_r \times N_t},$$

$$\hat{\mathbf{V}} = \mathbf{U}_j^{(n)} \mathbf{H}_j \triangleq \hat{\mathbf{V}}_j^{(n)} \in \mathcal{C}^{N_r \times N_t},$$

$$\mathbf{Y} = \mathbf{I} + \sum_{k=j+1}^K \mathbf{H}_k^H \mathbf{U}_k^H \mathbf{U}_k \mathbf{H}_k = \mathbf{I} + \sum_{k=j+1}^K \mathbf{V}_k^H \mathbf{V}_k \triangleq \mathbf{Y}_j$$

and

$$\begin{aligned} \hat{\mathbf{Y}} &= \mathbf{I} + \sum_{k=j+1}^K \mathbf{H}_k^H \mathbf{U}_k^{(n)H} \mathbf{U}_k^{(n)} \mathbf{H}_k \\ &= \mathbf{I} + \sum_{k=j+1}^K \hat{\mathbf{V}}_k^{(n)H} \hat{\mathbf{V}}_k^{(n)} \triangleq \hat{\mathbf{Y}}_j^{(n)} \in \mathcal{C}^{N_t \times N_t}. \end{aligned}$$

Then (19) implies

$$\begin{aligned} h(\mathbf{U}) &\geq \bar{h}(\mathbf{U}; \mathbf{U}^{(n)}) = c^{(n)} + \sum_{j=1}^K 2\Re \left(\text{Tr}(\mathbf{B}_j^{(n)} \mathbf{U}_j^H) \right) \\ &\quad - \sum_{j=1}^K \text{Tr}(\mathbf{A}_j^{(n)H} \sum_{k=j}^K \mathbf{H}_k^H \mathbf{U}_k^H \mathbf{U}_k \mathbf{H}_k). \end{aligned} \quad (20)$$

Algorithm 1: Optimization of the covariance matrices in the dual MAC.

Input: \mathbf{H} , \mathbf{S} , $\lambda^{(0)} \geq 0$, $n \leftarrow 0$

- 1 **repeat**
- 2 **for** $j = 1, 2, \dots, K$ **do**
- 3 Calculate $\hat{\mathbf{V}}_j^{(n)}$, $\hat{\mathbf{Y}}_j^{(n)}$, $\mathbf{A}_j^{(n)}$, $\mathbf{B}_j^{(n)}$
- 4 Decompose $\mathbf{H}_j \sum_{l=1}^j \mathbf{A}_l^{(n)} \mathbf{H}_j^H = \mathbf{P}_j \boldsymbol{\Sigma}_j \mathbf{P}_j^H$
- 5 **end**
- 6 Solve for λ_D in (30)
- 7 Compute $\mathbf{U}_j^{(n+1)}$ using (27) for $j = 1, 2, \dots, K$
- 8 $\lambda^{(n+1)} \leftarrow \lambda_D$
- 9 $n \leftarrow n + 1$
- 10 **until** $\lambda^{(n)} - \lambda^{(n-1)} > \epsilon_D$
- 11 Calculate all $\mathbf{S}_k^* = \mathbf{U}_k^{(n)H} \mathbf{U}_k^{(n)}$
- 12 **if** $\sum_{k=1}^K \text{Tr}(\mathbf{S}_k^*) \leq P$ **then**
- 13 $\mathbf{S}_{\text{opt}} = \mathbf{S}^*$
- 14 **else**
- 15 $\mathbf{S}_{\text{opt}} = \hat{\mathbf{S}}$ obtained from [23]
- 16 **end**

where

$$\begin{aligned}
c^{(n)} &= \sum_{j=1}^K \left[\ln \left| \mathbf{I} + \hat{\mathbf{V}}_j^{(n)} \left(\hat{\mathbf{Y}}_j^{(n)} \right)^{-1} \hat{\mathbf{V}}_j^{(n)H} \right| \right. \\
&\quad \left. - \text{Tr} \left(\hat{\mathbf{V}}_j^{(n)} \left(\hat{\mathbf{Y}}_j^{(n)} \right)^{-1} \hat{\mathbf{V}}_j^{(n)H} \right) - \text{Tr} \left(\mathbf{A}_j^{(n)H} \right) \right] \\
&= h(\mathbf{U}^{(n)}) - \sum_{j=1}^K \text{Tr} \left(\hat{\mathbf{V}}_j^{(n)} \left(\hat{\mathbf{Y}}_j^{(n)} \right)^{-1} \hat{\mathbf{V}}_j^{(n)H} \right) - \text{Tr} \left(\mathbf{A}_j^{(n)H} \right) \\
\mathbf{B}_j^{(n)} &= \bar{\mathbf{B}}_j^{(n)} \mathbf{H}_j^H \in \mathbb{C}^{N_r \times N_r}; \bar{\mathbf{B}}_j^{(n)} = \hat{\mathbf{V}}_j^{(n)} \left(\hat{\mathbf{Y}}_j^{(n)} \right)^{-1} \in \mathbb{C}^{N_r \times N_t} \\
\mathbf{A}_j^{(n)} &= \left(\hat{\mathbf{Y}}_j^{(n)} \right)^{-1} - \left(\hat{\mathbf{V}}_j^{(n)H} \hat{\mathbf{V}}_j^{(n)} + \hat{\mathbf{Y}}_j^{(n)} \right)^{-1} \\
&= \left(\hat{\mathbf{Y}}_j^{(n)} \right)^{-1} - \left(\hat{\mathbf{Y}}_{j-1}^{(n)} \right)^{-1} \in \mathbb{C}^{N_t \times N_t}.
\end{aligned}$$

Regarding the complexity of the above approximation, the following remark is in order.

Remark 1. Since $\hat{\mathbf{Y}} \in \mathbb{C}^{N_t \times N_t}$, it may appear that the complexity of constructing the above bound is $\mathcal{O}(N_t^3)$ due to the computation of $\left(\hat{\mathbf{Y}}_j^{(n)} \right)^{-1}$. However, we emphasize that this is not the case. Specifically, by invoking the matrix-inversion lemma we can write

$$\left(\hat{\mathbf{Y}}_j^{(n)} \right)^{-1} = \left(\hat{\mathbf{V}}_{j+1}^{(n)H} \hat{\mathbf{V}}_{j+1}^{(n)} + \hat{\mathbf{Y}}_{j+1}^{(n)} \right)^{-1} \quad (21)$$

$$= \left(\hat{\mathbf{Y}}_{j+1}^{(n)} \right)^{-1} - \left(\hat{\mathbf{Y}}_{j+1}^{(n)} \right)^{-1} \hat{\mathbf{V}}_{j+1}^{(n)H} \left(\mathbf{I} + \right. \quad (22)$$

$$\left. \hat{\mathbf{V}}_{j+1}^{(n)} \left(\hat{\mathbf{Y}}_{j+1}^{(n)} \right)^{-1} \hat{\mathbf{V}}_{j+1}^{(n)H} \right)^{-1} \hat{\mathbf{V}}_{j+1}^{(n)} \left(\hat{\mathbf{Y}}_{j+1}^{(n)} \right)^{-1} \quad (23)$$

$$= \left(\hat{\mathbf{Y}}_{j+1}^{(n)} \right)^{-1} - \bar{\mathbf{B}}_{j+1}^{(n)H} \left(\mathbf{I} + \bar{\mathbf{B}}_{j+1}^{(n)} \hat{\mathbf{V}}_{j+1}^{(n)H} \right)^{-1} \bar{\mathbf{B}}_{j+1}^{(n)}, \quad (24)$$

for $j = 1, 2, \dots, K-1$. The above equation indeed suggests a recursive method to compute $\left(\hat{\mathbf{Y}}_j^{(n)} \right)^{-1}$ efficiently. Suppose the inverse of $\hat{\mathbf{Y}}_{j+1}^{(n)}$ is known. Then, we only need to compute the inverse of the matrix $\mathbf{I} + \bar{\mathbf{B}}_{j+1}^{(n)} \hat{\mathbf{V}}_{j+1}^{(n)H} \in \mathbb{C}^{N_r \times N_r}$, which has complexity of $\mathcal{O}(N_r^3)$, to obtain $\left(\hat{\mathbf{Y}}_j^{(n)} \right)^{-1}$. Thus, starting

from $\hat{\mathbf{Y}}_K^{(n)} = \mathbf{I}$, we can iteratively compute $\left(\hat{\mathbf{Y}}_j^{(n)} \right)^{-1}$ for $j = K-1, K-2, \dots, 1$. In this way, $\mathbf{A}_j^{(n)}$ is also obtained easily.

Now, using the above lower bound of $h(\mathbf{U})$, we arrive at the following approximate problem

$$\underset{\mathbf{U}_k}{\text{maximize}} \frac{\bar{h}(\mathbf{U}; \mathbf{U}^{(n)})}{\sum_{k=1}^K \text{Tr}(\mathbf{U}_k^H \mathbf{U}_k) + N_t P_c + P_0 + L N P_s}. \quad (25)$$

3) *Dinkelbach's Method: Water-filling Solution:* It is important to note that (25) is a concave-convex fractional program since $\bar{h}(\mathbf{U}; \mathbf{U}^{(n)})$ is concave. Thus, Dinkelbach's method can be applied to find the optimal solution, which leads to the following parameterized problem

$$\begin{aligned}
\underset{\mathbf{U}_k}{\text{maximize}} f_{\lambda_D}(\mathbf{U}) &= c^{(n)} + \sum_{j=1}^K 2\Re \left(\text{Tr}(\mathbf{B}_j^{(n)} \mathbf{U}_j^H) \right) \\
&\quad - \sum_{j=1}^K \text{Tr} \left(\mathbf{A}_j^{(n)H} \sum_{k=j}^K \mathbf{H}_k^H \mathbf{U}_k^H \mathbf{U}_k \mathbf{H}_k \right) \\
&\quad - \lambda_D \left(\sum_{j=1}^K \text{Tr}(\mathbf{U}_j^H \mathbf{U}_j) + N_t P_c + P_0 + L N P_s \right) \quad (26)
\end{aligned}$$

where $\lambda_D > 0$ is a given parameter. Now it is straightforward to see that the above optimization problem can be solved independently for each \mathbf{U}_j , which admits the following closed-form solution

$$\mathbf{U}_j = \mathbf{B}_j^{(n)} \left(\mathbf{H}_j \sum_{l=1}^j \mathbf{A}_l^{(n)H} \mathbf{H}_j^H + \lambda_D \mathbf{I} \right)^{-1}, \quad j = 1, \dots, K. \quad (27)$$

Substituting (27) into (26) yields

$$\begin{aligned}
f_{\lambda_D}(\mathbf{U}) &= \sum_{j=1}^K \text{Tr} \left(\mathbf{B}_j^{(n)} \left(\mathbf{H}_j \sum_{l=1}^j \mathbf{A}_l^{(n)H} \mathbf{H}_j^H + \lambda_D \mathbf{I} \right)^{-1} \mathbf{B}_j^{(n)H} \right) \\
&\quad + c^{(n)} - \lambda_D \left(N_t P_c + P_0 + L N P_s \right) \quad (28)
\end{aligned}$$

Let $\mathbf{H}_j \sum_{l=1}^j \mathbf{A}_l^{(n)H} \mathbf{H}_j^H = \mathbf{P}_j \boldsymbol{\Sigma}_j \mathbf{P}_j^H$ be the eigenvalue decomposition of $\mathbf{H}_j \sum_{l=1}^j \mathbf{A}_l^{(n)H} \mathbf{H}_j^H$ where $\mathbf{P}_j \in \mathbb{C}^{N_r \times N_r}$ is unitary and $\boldsymbol{\Sigma}_j \in \mathbb{C}^{N_r \times N_r}$ is diagonal. Then, we can rewrite $f_{\lambda_D}(\mathbf{U})$ as

$$\begin{aligned}
f_{\lambda_D}(\mathbf{U}) &= \sum_{j=1}^K \text{Tr} \left(\mathbf{B}_j^{(n)} \mathbf{P}_j^H \left(\boldsymbol{\Sigma}_j + \lambda_D \mathbf{I} \right)^{-1} \mathbf{P}_j \mathbf{B}_j^{(n)H} \right) \\
&\quad + c^{(n)} + \lambda_D \left(N_t P_c + P_0 + L N P_s \right) \quad (29)
\end{aligned}$$

$$= \sum_{j=1}^K \sum_{i=1}^{N_r} \frac{d_{ji}}{\sigma_{ji} + \lambda_D} + c^{(n)} - \lambda_D \left(N_t P_c + P_0 + L N P_s \right) \quad (30)$$

where d_{ji} is the i th diagonal element of $\mathbf{P}_j^H \mathbf{B}_j^{(n)H} \mathbf{B}_j^{(n)} \mathbf{P}_j$ and σ_{ji} is the i th diagonal element of $\boldsymbol{\Sigma}_j$. Next, we need to find λ_D such that $f_{\lambda_D}(\mathbf{U}) = 0$, which can be solved using either the bisection method or Newton's method.

Let \mathbf{U}_k^* be the optimal solution to (25), which is returned by Dinkelbach's method described above. Then $\mathbf{S}_k^* = (\mathbf{U}_k^*)^\dagger \mathbf{U}_k^*$ is the optimal solution to (14), for $k = 1, \dots, K$. Obviously, if $\sum_{k=1}^K \text{Tr}(\mathbf{S}_k^*) \leq P_{\text{max}}$, then $\mathbf{S}^* = (\mathbf{S}_1^*, \mathbf{S}_2^*, \dots, \mathbf{S}_K^*)$ is also optimal to (11a). On the other hand, if $\sum_{k=1}^K \text{Tr}(\mathbf{S}_k^*) > P_{\text{max}}$,

it is straightforward to see that the optimal solution to (11a) is obtained by solving the sum-rate maximization problem with the sum power constraint, which is defined as:

$$\underset{\mathbf{S}_k}{\text{maximize}} \ln \left| \mathbf{I} + \sum_{k=1}^K \mathbf{H}_k^H \mathbf{S}_k \mathbf{H}_k \right| \quad (31a)$$

$$\text{subject to } \text{Tr}(\mathbf{S}_k) \leq P_{\max}. \quad (31b)$$

An efficient method for solving the above problem was proposed in [23], which we omit the details for the sake of brevity. Let $\hat{\mathbf{S}} = (\hat{\mathbf{S}}_1, \hat{\mathbf{S}}_2, \dots, \hat{\mathbf{S}}_K)$ be the optimal solution to (31). Then it is easy to see that the optimal covariance matrices for (13) are given by

$$\mathbf{S}_{\text{opt}} = \begin{cases} \mathbf{S}^* & \sum_{k=1}^K \text{Tr}(\mathbf{S}_k^*) \leq P_{\max} \\ \hat{\mathbf{S}} & \text{otherwise.} \end{cases} \quad (32)$$

A summary of the described covariance matrix optimization method is presented in **Algorithm 1**.

B. SIM Phase Shift Optimization

Since the total power consumption does not depend on the SIM phase shifts, the SIM phase shift optimization problem for fixed \mathbf{S} is formulated as

$$\underset{\phi}{\text{maximize}} \quad \kappa(\phi) = \ln \left| \mathbf{I} + \sum_{k=1}^K \mathbf{H}_k^H \mathbf{S}_k \mathbf{H}_k \right| \quad (33a)$$

$$\text{subject to} \quad |\phi_n^l| = 1, \forall l, n. \quad (33b)$$

Considering the large size of the SIM, we adopt a gradient-based method to optimize the phase shifts, which consists of the following iterations:

$$\phi^{(n+1)} = \mathcal{P}_\phi(\phi^{(n)} + u_n \nabla_{\phi} \kappa(\phi^{(n)})), \quad (34)$$

where $\mathcal{P}_\phi(\cdot)$ denotes the projection operator that ensures the unit modulus constraint on ϕ and u_n is the appropriate step size. The gradient of $\kappa(\phi)$ w.r.t. the phase shifts of the SIM is determined by the gradients of $\kappa(\phi)$ w.r.t. the phase shifts of the constituent SIM layers as

$$\nabla_{\phi} \kappa(\phi) = [\nabla_{\phi^1} \kappa(\phi)^T \dots \nabla_{\phi^L} \kappa(\phi)^T]^T.$$

The gradient w.r.t. each ϕ^L is provided in Theorem 1.

Theorem 1. *The gradient of $h(\phi)$ w.r.t. ϕ^L is given by*

$$\nabla_{\phi^l} \kappa(\phi) = \text{vec}_d(\mathbf{C}) \quad (35)$$

where

$$\mathbf{D} = \mathbf{I} + \sum_{k=1}^K \mathbf{H}_k^H \mathbf{S}_k \mathbf{H}_k \quad (36a)$$

$$\mathbf{C} = \Theta^{l+1:L} \sum_{k=1}^K \mathbf{G}_k^H \mathbf{S}_k \mathbf{H}_k \mathbf{D}^{-1} \Theta^{1:l-1} (\mathbf{W}^l)^H \quad (36b)$$

where $\Theta^{m:n} = (\mathbf{W}^m)^H (\Phi^m)^H \dots (\mathbf{W}^n)^H (\Phi^n)^H$.

Proof: By differentiating $\kappa(\phi)$ w.r.t. Φ^l , we obtain

$$\begin{aligned} d\kappa(\phi) &= \text{Tr} \left(\mathbf{D}^{-1} \sum_{k=1}^K d(\mathbf{H}_k^H \mathbf{S}_k \mathbf{H}_k) \right) = \\ &= \text{Tr} \left(\sum_{k=1}^K \mathbf{S}_k \mathbf{H}_k \mathbf{D}^{-1} d\mathbf{H}_k^H + \sum_{k=1}^K \mathbf{D}^{-1} \mathbf{H}_k^H \mathbf{S}_k d\mathbf{H}_k \right). \end{aligned} \quad (37)$$

Algorithm 2: Proposed algorithm for the EE optimization for a SIM-aided broadcast system with DPC precoding.

Input: $\mathbf{H}, \mathbf{S}^{(0)}, \phi^{(0)}, \delta > 0, u_0 > 0, \rho \in (0, 1), n \leftarrow 0$

- 1 **repeat**
- 2 Call **Algorithm 1** to obtain $\mathbf{S}^{(n+1)}$
- 3 **repeat**
- 4 $\phi^{(n+1)} = \mathcal{P}_\phi(\phi^{(n)} + u_n \nabla_{\phi} \kappa(\phi^{(n)}))$
- 5 **if** $\kappa(\phi^{(n+1)}) < \kappa(\phi^{(n)}) + \delta \|\phi^{(n+1)} - \phi^{(n)}\|^2$
- 6 **then**
- 7 $u_n \leftarrow \rho u_n$
- 8 **end**
- 9 **until** $\kappa(\phi^{(n+1)}) \geq \kappa(\phi^{(n)}) + \delta \|\phi^{(n+1)} - \phi^{(n)}\|^2$
- 10 Calculate \mathbf{B} and \mathbf{H} for $\phi^{(n+1)}$
- 11 $u_{n+1} \leftarrow u_n$
- 12 $n \leftarrow n + 1$
- 13 **until** convergence of η_{dpc} in (11a)

After \mathbf{S}_{opt} is obtained, optimal covariance matrices in the BC are found using the BCs-MACs duality.

Substituting

$$d\mathbf{H}_k = \mathbf{G}_k \Phi^L \mathbf{W}^L \dots d\Phi^l \mathbf{W}^l \dots \Phi^1 \mathbf{W}^1 \quad (38)$$

in the previous equation results in

$$d\kappa(\phi) = \text{Tr}(\mathbf{C} d(\Phi^l)^H + \mathbf{C}^H d\Phi^l) \quad (39)$$

where \mathbf{C} is defined in (36b). Hence, we have

$$\nabla_{\Phi^l} \kappa(\phi) = \mathbf{C} \quad (40)$$

and using $\Phi^l = \text{diag}(\phi^l)$, we obtain (35). \blacksquare

Since all the elements of ϕ have unit amplitude, the projection $\mathcal{P}_\phi(\phi)$ is defined by

$$\bar{\phi}_n^l = \begin{cases} \phi_n^l / |\phi_n^l| & \phi_n^l \neq 0, \\ e^{j\alpha}, \alpha \in [0, 2\pi] & \phi_n^l = 0. \end{cases} \quad (41)$$

The initial step size u_0 is chosen as an arbitrary large positive number. Later, the step size in the n -th iteration of the proposed algorithm u_n can be expressed as $u_0 \rho^{k_n}$, where $k_n \geq 0$ is the smallest integer that satisfies $\kappa(\phi^{(n+1)}) \geq \kappa(\phi^{(n)}) + \delta \|\phi^{(n+1)} - \phi^{(n)}\|^2$, where $\delta > 0$ is a small constant and $\rho \in (0, 1)$.

Finally, the EE optimization algorithm for a SIM-aided broadcast system with DPC precoding is given in **Algorithm 2**.

IV. PROPOSED SOLUTION TO LP

In this section, we propose an optimization method for the EEmax problem with LP. Similar to the previous section, the precoding matrices are found in closed-form using Dinkelbach's method, which also yields a water-filling solution. The phase shifts for the SIM meta-elements are optimized by a gradient-based method.

A. Precoding Matrix Optimization

For fixed ϕ , the precoding matrix optimization in (12) reduces to the EEmax problem in conventional MIMO systems. The structure of our proposed method for precoding matrix optimization as follows:

- Reduce the dimension of the precoding matrix optimization problem by considering an equivalent reformulation.
- Apply (19) to obtain a lower bound of the achievable rate for LP.
- Adopt Dinkelbach's method to solve the attained problem, which leads to water-filling solution.

1) *Problem Reformulation: Dimension Reduction:* It can be observed that the complexity of the direct optimization of \mathbf{P} is proportional to N_t , which can cause a significant complexity burden even for moderate values of N_t . Consequently, such a direct optimization method is not practically appealing.

To overcome this issue, we consider an equivalent formulation of (12), introduced in [24], which reduces the problem's size and computational complexity. Denoting $\mathbf{H} = [\mathbf{H}_1^T \mathbf{H}_2^T \dots \mathbf{H}_K^T]^T \in \mathbb{C}^{KN_r \times N_t}$, (12) can be equivalently written as

$$\underset{\mathbf{X}}{\text{maximize}} f(\mathbf{X}) = \frac{\sum_{k=1}^K \bar{R}_k}{\sum_{k=1}^K \text{Tr}(\bar{\mathbf{H}}\mathbf{X}_k\mathbf{X}_k^H) + N_t P_c + P_0 + LNP_s} \quad (42a)$$

$$\text{subject to } \sum_{k=1}^K \text{Tr}(\bar{\mathbf{H}}\mathbf{X}_k\mathbf{X}_k^H) \leq P_{\max}, \quad (42b)$$

where

$$\bar{R}_k = \ln \left| \mathbf{I} + \bar{\mathbf{H}}_k \mathbf{X}_k \mathbf{X}_k^H \bar{\mathbf{H}}_k^H \left(\mathbf{I} + \sum_{j=1, j \neq k}^K \bar{\mathbf{H}}_j \mathbf{X}_j \mathbf{X}_j^H \bar{\mathbf{H}}_j^H \right) \right| \quad (43)$$

$\mathbf{X} = [\mathbf{X}_1 \mathbf{X}_2 \dots \mathbf{X}_K] \in \mathbb{C}^{KN_r \times KN_r}$ are new optimization variables, and $\bar{\mathbf{H}}_k = \mathbf{H}_k \mathbf{H}_k^H \in \mathbb{C}^{N_r \times KN_r}$ is the k -th submatrix of $\bar{\mathbf{H}} = \mathbf{H}\mathbf{H}^H \in \mathbb{C}^{KN_r \times KN_r}$. The equivalence between (12) and (42) is a result of [24, Prop. 2], and the optimal solutions of the two problems are related as $\mathbf{P}_k = \mathbf{H}^H \mathbf{X}_k$. When comparing the size of \mathbf{X} and $\mathbf{P} = [\mathbf{P}_1, \mathbf{P}_2, \dots, \mathbf{P}_K] \in \mathbb{C}^{N_t \times KN_r}$, we see that the equivalent formulation in (42) significantly reduces the number of optimization variables, particularly for systems with large N_t (i.e., $N_t \gg N_r$). Following a similar approach as in **Algorithm 1**, we first derive a solution for the unconstrained case by dropping (42b), with the solution for the constrained case following immediately.

2) *SCA Method: A Tight Lower Bound of Sum Rate:* Upon close inspection, we observe that the denominator of (42) is a quadratic convex function, while the numerator of (42) is neither a convex nor concave function. As a result, solving (42) is nontrivial. To develop an efficient solution, we again exploit the inequality, given in (19), to obtain a lower bound of the achievable rate in (43). Using the identity $|\mathbf{I} + \mathbf{Z}_k \mathbf{Z}_k^H \mathbf{Y}_k| =$

$|\mathbf{I} + \mathbf{Z}_k^H \mathbf{Y}_k \mathbf{Z}_k|$ to reformulate (43), the lower bound of the achievable rate of user k can be expressed as

$$\begin{aligned} \bar{R}_k &\geq L_k = \ln \left| \mathbf{I} + \hat{\mathbf{Z}}_k^H \hat{\mathbf{Y}}_k^{-1} \hat{\mathbf{Z}}_k \right| - \text{Tr}(\hat{\mathbf{Z}}_k^H \hat{\mathbf{Y}}_k^{-1} \hat{\mathbf{Z}}_k) \\ &\quad + 2\Re(\text{Tr}(\hat{\mathbf{Z}}_k^H \hat{\mathbf{Y}}_k^{-1} \bar{\mathbf{H}}_k \mathbf{X}_k)) \\ &\quad - \sum_{j=1}^K \text{Tr}(\mathbf{X}_j^H \bar{\mathbf{H}}_j^H \mathbf{A}_k^H \bar{\mathbf{H}}_j \mathbf{X}_j) - \text{Tr}(\mathbf{A}_k^H) \end{aligned} \quad (44)$$

where $\mathbf{Z}_k = \bar{\mathbf{H}}_k \mathbf{X}_k \in \mathbb{C}^{N_r \times N_r}$, $\hat{\mathbf{Z}}_k = \bar{\mathbf{H}}_k \mathbf{X}_k^{(n)} \in \mathbb{C}^{N_r \times N_r}$, $\mathbf{Y}_k = \sum_{j=1, j \neq k}^K \bar{\mathbf{H}}_j \mathbf{X}_j \mathbf{X}_j^H \bar{\mathbf{H}}_j^H + \mathbf{I} \in \mathbb{C}^{N_r \times N_r}$, $\hat{\mathbf{Y}}_k = \sum_{j=1, j \neq k}^K \bar{\mathbf{H}}_j \mathbf{X}_j^{(n)} (\mathbf{X}_j^{(n)})^H \bar{\mathbf{H}}_j^H + \mathbf{I} \in \mathbb{C}^{N_r \times N_r}$, $\mathbf{A}_k = \hat{\mathbf{Y}}_k^{-1} - (\hat{\mathbf{Z}}_k \hat{\mathbf{Z}}_k^H + \hat{\mathbf{Y}}_k)^{-1} \in \mathbb{C}^{N_r \times N_r}$, and $\mathbf{X}_k^{(n)}$ represents the value of \mathbf{X}_k at the n -th iteration. Consequently, the resulting approximate problem of (42) is given by

$$\underset{\mathbf{X}}{\text{maximize}} \bar{f}(\mathbf{X}) = \frac{\sum_{k=1}^K L_k}{\sum_{k=1}^K \text{Tr}(\bar{\mathbf{H}}\mathbf{X}_k\mathbf{X}_k^H) + N_t P_c + P_0 + LNP_s} \quad (45)$$

which is a concave-convex optimization problem.

3) *Dinkelbach's method: Closed-form Solution:* Next, we apply Dinkelbach's method to solve (45), leading to the following optimization problem

$$\underset{\mathbf{X}}{\text{maximize}} M_{\lambda_L}(\mathbf{X}) \quad (46)$$

where

$$\begin{aligned} M_{\lambda_L}(\mathbf{X}) &= \sum_{k=1}^K L_k - \lambda_L \left(\sum_{k=1}^K \text{Tr}(\bar{\mathbf{H}}\mathbf{X}_k\mathbf{X}_k^H) \right. \\ &\quad \left. + N_t P_c + P_0 + LNP_s \right) \end{aligned} \quad (47)$$

and $\lambda_L \geq 0$ is a given parameter.

Applying the Karush-Kuhn-Tucker (KKT) first-order optimality condition to (46), we take the gradient w.r.t. \mathbf{X}_j^* and set it to $\mathbf{0}$, giving

$$\left(\hat{\mathbf{Z}}_j^H \hat{\mathbf{Y}}_j^{-1} \bar{\mathbf{H}}_j \right)^H - \sum_{k=1}^K \bar{\mathbf{H}}_k^H \mathbf{A}_k^H \bar{\mathbf{H}}_k \mathbf{X}_j - \lambda_L \bar{\mathbf{H}} \mathbf{X}_j = \mathbf{0} \quad (48)$$

To solve for \mathbf{X}_j we differentiate two cases. If \mathbf{H} is a row-rank matrix, e.g. (i.e., $KN_r < N_t$), then $\bar{\mathbf{H}}$ is invertible, and thus (48) results in

$$\mathbf{X}_j = \left(\sum_{k=1}^K \bar{\mathbf{H}}_k^H \mathbf{A}_k^H \bar{\mathbf{H}}_k + \lambda_L \bar{\mathbf{H}} \right)^{-1} \bar{\mathbf{H}}_j^H \hat{\mathbf{Y}}_j^{-1} \hat{\mathbf{Z}}_j. \quad (49)$$

If \mathbf{H} is column-rank matrix (i.e., $KN_r > N_t$), we rewrite (48) as

$$\mathbf{H} \left(\mathbf{H}_j^H \hat{\mathbf{Y}}_j^{-1} \hat{\mathbf{Z}}_j - \sum_{k=1}^K \mathbf{H}_k^H \mathbf{A}_k^H \bar{\mathbf{H}}_k \mathbf{X}_j - \lambda_L \mathbf{H}^H \mathbf{X}_j \right) = \mathbf{0} \quad (50)$$

and finally obtain

$$\mathbf{X}_j = \left(\sum_{k=1}^K \mathbf{H}_k^H \mathbf{A}_k^H \bar{\mathbf{H}}_k + \lambda_L \mathbf{H}^H \right)^+ \mathbf{H}_j^H \hat{\mathbf{Y}}_j^{-1} \hat{\mathbf{Z}}_j. \quad (51)$$

If the solution obtained from (49) or (51) satisfies the power constraint (42b), then it is also the optimal solution to (42). Otherwise, the optimal \mathbf{X} is determined by solving the achievable sum rate optimization problem

$$\underset{\mathbf{X}}{\text{maximize}} \sum_{k=1}^K \bar{R}_k \quad (52a)$$

$$\text{subject to } \sum_{k=1}^K \text{Tr}(\bar{\mathbf{H}}\mathbf{X}_k\mathbf{X}_k^H) \leq P_{\max}, \quad (52b)$$

Algorithm 3: Optimization of the precoding matrices.

Input: \mathbf{H} , $\mathbf{X}^{(0)}$, ϕ , $\lambda_L^{(0)} \geq 0$, $m \leftarrow 0$

- 1 **repeat**
- 2 $n \leftarrow 0$
- 3 **repeat**
- 4 Calculate all $\hat{\mathbf{Z}}_k$, $\hat{\mathbf{Y}}_k$, \mathbf{A}_k
- 5 Calculate \mathbf{X}_{opt} according to (49) or (51)
- 6 $\mathbf{X}^{(n+1)} \leftarrow \mathbf{X}_{\text{opt}}$
- 7 $n \leftarrow n + 1$
- 8 **until** $\lambda_L^{(m+1)} - \lambda_L^{(m)} > \epsilon_{2,L}$
- 9 $\lambda_L^{(m+1)} \leftarrow f(\mathbf{X}^{(n)})$ according to (42a)
- 10 $m \leftarrow m + 1$
- 11 $\mathbf{X}^{(0)} \leftarrow \mathbf{X}^{(n)}$
- 12 **until** $f(\mathbf{X}^{(n+1)}) - f(\mathbf{X}^{(n)}) > \epsilon_{1,L}$
- 13 **if** $\sum_{k=1}^K \text{Tr}(\bar{\mathbf{H}}\mathbf{X}_k\mathbf{X}_k^H) \leq P_{\text{max}}$ **then**
- 14 $\mathbf{X}_{\text{opt}} = \mathbf{X}$
- 15 **else**
- 16 \mathbf{X}_{opt} obtained from [24]
- 17 **end**
- 18 **for** $k = 1$ **to** K **do**
- 19 $\mathbf{P}_k = \mathbf{H}^H \mathbf{X}_{\text{opt},k}$
- 20 **end**

Algorithm 4: Proposed algorithm for the EE optimization for a SIM-aided broadcast system with LP.

Input: \mathbf{H} , $\mathbf{X}^{(0)}$, $\phi^{(0)}$, $\lambda^{(0)} \geq 0$, $\delta > 0$, $t_n > 0$, $\rho \in (0, 1)$, $n \leftarrow 0$

- 1 **repeat**
- 2 Call **Algorithm 3** to obtain $\mathbf{P}^{(n+1)}$
- 3 **repeat**
- 4 $\phi^{(n+1)} = \mathcal{P}_\phi(\phi^{(n)} + t_n \nabla_\phi \tau(\phi^{(n)}))$
- 5 **if** $\tau(\phi^{(n+1)}) < \tau(\phi^{(n)}) + \delta \|\phi^{(n+1)} - \phi^{(n)}\|^2$ **then**
- 6 $t_n \leftarrow \rho t_n$
- 7 **end**
- 8 **until** $\tau(\phi^{(n+1)}) \geq \tau(\phi^{(n)}) + \delta \|\phi^{(n+1)} - \phi^{(n)}\|^2$
- 9 $n \leftarrow n + 1$
- 10 **until** convergence of η_{lp} in (12a)

which can be solved by [24, Algorithm 1]. The described optimization algorithm is summarized in **Algorithm 3**.

B. SIM Phase Shift Optimization

For a fixed \mathbf{P} , the SIM phase shift optimization problem is formulated as

$$\underset{\phi}{\text{maximize}} \quad \tau(\phi) = \sum_{k=1}^K R_{L,k}(\phi) \quad (53a)$$

$$\text{subject to} \quad |\phi_n^l| = 1, \forall l, n, \quad (53b)$$

where we have used the rate expression in (8) instead of (43). This choice not only simplifies the gradient computation of the objective function w.r.t ϕ but also leads to faster convergence rate as explained in [25].

The optimization of the phase shifts of the BS SIM follows the same steps as in the case of DPC discussed in subsection III-B. Specifically, the phase shifts are iteratively updated according to

$$\phi^{(n+1)} = \mathcal{P}_\phi(\phi^{(n)} + t_n \nabla_\phi \tau(\phi^{(n)})), \quad (54)$$

where t_n is the appropriate step size. Also, the gradient $\nabla_\phi \tau(\phi)$ is given by $\nabla_\phi \tau(\phi) = [\nabla_{\phi^1} \tau(\phi)^T \cdots \nabla_{\phi^L} \tau(\phi)^T]^T$, where $\nabla_{\phi^l} \tau(\phi)$ is expressed in the following theorem.

Theorem 2. The gradients of $\tau(\phi)$ w.r.t. the l -th layer of the SIM at the BS is given by

$$\begin{aligned} \nabla_{\phi^l} \tau(\phi) = & \text{vec}_d \left(\sum_{k=1}^K \Theta^{l+1:L} \mathbf{G}_k^H \mathbf{F}_{1,k}^{-1} \mathbf{H}_k \hat{\mathbf{P}}_s \Theta^{1:l-1} \mathbf{W}_l^H \right) \\ & - \text{vec}_d \left(\sum_{k=1}^K \Theta^{l+1:L} \mathbf{G}_k^H \mathbf{F}_{2,k}^{-1} \mathbf{H}_k \hat{\mathbf{P}}_k \Theta^{1:l-1} \mathbf{W}_l^H \right) \end{aligned} \quad (55)$$

where $\Theta^{m:n} = (\mathbf{W}^m)^H (\Phi^m)^H \cdots (\mathbf{W}^n)^H (\Phi^n)^H$, $\hat{\mathbf{P}}_s = \sum_{j=1}^K \mathbf{P}_j \mathbf{P}_j^H$, $\hat{\mathbf{P}}_k = \sum_{j=1, j \neq k}^K \mathbf{P}_j \mathbf{P}_j^H$, $\mathbf{F}_{1,k} = \mathbf{I} + \mathbf{H}_k \hat{\mathbf{P}}_s \mathbf{H}_k^H$ and $\mathbf{F}_{2,k} = \mathbf{I} + \mathbf{H}_k \hat{\mathbf{P}}_k \mathbf{H}_k^H$.

Proof: See the Appendix. ■

The outline of the proposed algorithm is given in **Algorithm 4**.

V. COMPUTATIONAL COMPLEXITY

In this section, the computational complexity for SIM-aided broadcast systems with DPC and LP is obtained by counting the required number of complex multiplications. In the following complexity analysis, for simplicity, we assume that $N, N_t \gg N_r$ which is a typical case for a SIM-based broadcast communication system.

A. DPC Precoding

The covariance matrix optimization is performed by **Algorithm 1**, with the complexity of obtaining \mathbf{U} from \mathbf{S} being negligible. In addition, the complexity of one iteration of inner loop (i.e., lines 2 to 5 in **Algorithm 1**) is $\mathcal{O}(N_t^2 N_r)$. Also, the complexity of line 6 is approximately $\mathcal{O}(K N_t N_r^2)$, while the complexity of line 7 can be neglected. Let I_U denote the number of inner loops (i.e., lines 1 to 1 in **Algorithm 1**), then the complexity of **Algorithm 1** is given by $\mathcal{O}(I_U K N_t^2 N_r)$.

Optimizing the SIM phase shifts requires $\mathcal{O}(K N N_t N_r)$ multiplications for computing $\sum_{k=1}^K \mathbf{G}_k^H \mathbf{S}_k \mathbf{H}_k$. The matrix inversion \mathbf{A}^{-1} and its multiplication contribute $\mathcal{O}(N_t^3 + N N_t^2)$ multiplications. Since $(\mathbf{W}^m)^H (\Phi^m)^H$ is precomputed and only the diagonal elements are needed in (35), the additional complexity is $\mathcal{O}(L N^3)$. Hence, the complexity of the gradient calculation is $\mathcal{O}(N N_t^2 + L N^3)$. After obtaining $\phi^{(n+1)}$, the complexity of calculating \mathbf{B} and \mathbf{H} is $\mathcal{O}(L N^3)$. In addition, $\mathcal{O}(K N_t N_r (N_t + N_r) + N_t^3) \approx \mathcal{O}(N_t^3)$ multiplications are needed to obtain $h(\phi^{(n+1)})$. The complexity of the SIM phase shifts optimization is $\mathcal{O}(N N_t^2 + I_{\phi,D} (L N^3 + N_t^3))$, where $I_{\phi,D}$ is the number of line search iterations.

Therefore, the overall computational complexity for single iteration of **Algorithm 2** is given by

$$C_{\text{SIM-DPC}} = \mathcal{O}(I_U K N_t^2 N_r + N N_t^2 + I_{\phi,D} (L N^3 + N_t^3)). \quad (56)$$

B. Linear Precoding (LP)

The optimization of the precoding matrices follows **Algorithm 3**, where computing \mathbf{H} requires $\mathcal{O}(K^2 N_t N_r^2)$ multiplications. Computing the initial \mathbf{X} from \mathbf{P} requires $\mathcal{O}(K^2 N_t N_r^2 + K^3 N_r^3)$ multiplications. Furthermore, the complexity of calculating all $\hat{\mathbf{Z}}_k$, $\hat{\mathbf{Y}}_k$ and \mathbf{A}_k is $\mathcal{O}(K^3 N_r^3 + K^2 N_r^3)$. To determine \mathbf{X} ,

- if $N_t \geq KN_r$, solving (49) requires $\mathcal{O}(K^3 N_r^3)$ multiplications, or otherwise according to
- if $N_t < KN_r$, solving (51) requires $\mathcal{O}(K^3 N_r^3 + K^3 N_t N_r^2) \approx \mathcal{O}(K^3 N_t N_r^2)$ multiplications.

Thus, the computational complexity of precoding matrix optimization is written as

$$C_x = \begin{cases} \mathcal{O}(K^3 N_r^3) & N_t \geq KN_r \\ \mathcal{O}(K^3 N_t N_r^2) & N_t < KN_r. \end{cases} \quad (57)$$

The complexity for calculating $\sum_k \bar{R}_k$ and $f(\mathbf{X}^{(n)})$ can be neglected. Let I_X denote the number of inner loops (i.e., lines 3 to 8 in **Algorithm 3**), then the complexity of **Algorithm 3** is given by $\mathcal{O}(I_X C_x)$.

To optimize the phase shifts of the SIM, we need $\mathcal{O}(KN_t^2)$ multiplications to obtain $\hat{\mathbf{P}}_s$ and all $\hat{\mathbf{P}}_k$ matrices, while calculating $\mathbf{F}_{1,k}$ and $\mathbf{F}_{2,k}$ requires $\mathcal{O}(KN_t N_r (N_t + N_r))$ multiplications, which also holds for $\mathbf{F}_{1,k}^{-1} \mathbf{H}_k \hat{\mathbf{P}}_s - \mathbf{F}_{2,k}^{-1} \mathbf{H}_k \hat{\mathbf{P}}_k$. Multiplying these terms with \mathbf{G}_k^H adds $\mathcal{O}(KNN_t^2)$ multiplications. As mentioned earlier, since $(\mathbf{W}^m)^H (\Phi^m)^H$ are precomputed and only the diagonal elements are need in (55), the additional complexity is $\mathcal{O}(LN^3)$. Hence, the complexity of the gradient calculation is $\mathcal{O}(KNN_t^2 + LN^3)$. After obtaining $\phi^{(n+1)}$, the complexity of calculating \mathbf{B} and \mathbf{H} is $\mathcal{O}(LN^3)$. To obtain all terms $\sum_j \mathbf{H}_k \mathbf{P}_j \mathbf{P}_j^H \mathbf{H}_k^H$, we need $\mathcal{O}(KN_t N_r (N_t + N_r))$ multiplications. Any additional complexity for computing $g(\phi^{(n+1)})$ can be neglected. Hence, the complexity of optimizing the SIM phase shifts is $\mathcal{O}(KNN_t^2 + I_{\phi,L} LN^3)$, where $I_{\phi,L}$ is the number of line search steps.

Therefore, the overall computational complexity for one iteration of **Algorithm 4** is given by

$$C_{\text{SIM-LP}} = \mathcal{O}(I_X C_x + KNN_t^2 + I_{\phi,L} LN^3). \quad (58)$$

VI. CONVERGENCE

We now prove the convergence of **Algorithm 2**. First, for a given ϕ , **Algorithm 2** achieves monotonic convergence, which can be shown as follows. From (20), it holds that

$$g(\mathbf{U}^{(n+1)}) = \frac{h(\mathbf{U}^{(n+1)})}{\sum_{k=1}^K \text{Tr}(\mathbf{U}_k^{(n+1)H} \mathbf{U}_k^{(n+1)}) + N_t P_c + P_0 + LNP_s} \quad (59)$$

$$\stackrel{(a)}{\geq} \frac{\bar{h}(\mathbf{U}^{(n+1)}; \mathbf{U}^{(n)})}{\sum_{k=1}^K \text{Tr}(\mathbf{U}_k^{(n+1)H} \mathbf{U}_k^{(n+1)}) + N_t P_c + P_0 + LNP_s} \quad (60)$$

$$\stackrel{(b)}{\geq} \frac{\bar{h}(\mathbf{U}^{(n)}; \mathbf{U}^{(n)})}{\sum_{k=1}^K \text{Tr}(\mathbf{U}_k^{(n)H} \mathbf{U}_k^{(n)}) + N_t P_c + P_0 + LNP_s} \quad (61)$$

$$\stackrel{(c)}{\geq} \frac{h(\mathbf{U}^{(n)})}{\sum_{k=1}^K \text{Tr}(\mathbf{U}_k^{(n)H} \mathbf{U}_k^{(n)}) + N_t P_c + P_0 + LNP_s} = g(\mathbf{U}^{(n)}) \quad (62)$$

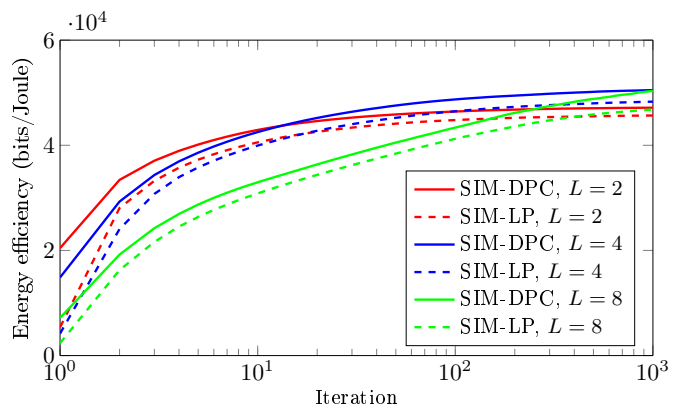


Fig. 2. Convergence of the proposed algorithms for different number of SIM layers.

where (a) follows from (20), (b) holds because $\mathbf{U}^{(n+1)}$ is the optimal solution to (25) and that the optimal objective is no less than the objective of a feasible point, and (c) is true because it is easy to check that $\bar{h}(\mathbf{U}^{(n)}; \mathbf{U}^{(n)}) = h(\mathbf{U}^{(n)})$, i.e. the equality in (20) occurs when $\mathbf{U} = \mathbf{U}^{(n)}$. Regarding (b) above, note again that since (25) is a concave-convex fractional program, Dinkelbach's method is guaranteed to converge to its optimal solution. Consequently, the sequence $\{g(\mathbf{U}^{(n)})\}$ increases monotonically to an optimal solution to (17), and thus, **Algorithm 2** is able to compute an optimal solution to (13). Next, for given covariance matrices, the SIM phase shift is optimized by a standard projected gradient method, for which the convergence is guaranteed. Also, the projected gradient method always yields an improved solution. In other words, **Algorithm 2** generates a non-decreasing objective sequence. Since the feasible sets for the covariance matrices and phase shifts are continuous, the objective sequence produced by **Algorithm 2** is guaranteed to converge.

Since **Algorithm 4** uses a similar method for the optimization of the precoding matrices, as **Algorithm 2** for the optimization of the covariance matrices, we can prove, following the same derivation steps, that for a given ϕ **Algorithm 4** is guaranteed to provide an optimal solution to (25). In addition, a gradient-based optimization of the SIM phase shifts always increase the objective function. Moreover, the feasible sets for the precoding matrices and phase shifts are continuous, which ensures the convergence of the objective sequence in **Algorithm 4**.

VII. SIMULATION RESULTS

In this section, we evaluate the EE of the proposed schemes with DPC and LP, which are denoted as SIM-DPC and SIM-LP, respectively, through Monte Carlo simulations and compare them with three benchmark schemes:

- 1) *LP-NoSIM*: The first benchmark scheme uses LP without SIM integration, with a total power consumption of $P_t + N_t P_c + P_0$.
- 2) *SIM-NoLP*: The second scheme, omits digital precoding, feeding data streams directly to transmit antennas while optimizing SIM phase shifts as in **Algorithm 4**. Let $N_{t,k}$ BS antennas are allocated for transmission to the k -th user. Since all N_t transmit antennas are active, $N_{t,k}$

equals $\lfloor N_t/K \rfloor$ or $\lfloor N_t/K \rfloor + 1$. Thus, each data stream of user k is transmitted by $\lfloor N_{t,k}/N_r \rfloor$ or $\lfloor N_{t,k}/N_r \rfloor + 1$ BS antennas.

- 3) *SIM-NoLP-RedRF*: The third scheme excludes LP but differs from SIM-NoLP by utilizing a reduced number of transmit antennas (i.e., RF chains). Specifically, it activates KN_r transmit antennas (i.e., RF chains), each transmitting an independent data stream, while the remaining transmit antennas remain inactive. As such, the total power consumption of $P_t + KN_r P_c + P_0 + LNP_s$. Note that for the case when $KN_r > N_t$, SIM-NoLP transmits signal to a subset of randomly chosen users, while LP-NoSIM-RedRF cannot operate. To ensure fair comparison, data for SIM-NoLP and LP-NoSIM-RedRF are scaled by $\sqrt{P_{\max}/N_t}$ and $\sqrt{P_{\max}/KN_r}$, respectively.

Channel Modeling: The channel matrix between the BS and user k is modeled as $\mathbf{G}_k = \bar{\mathbf{G}}_k \mathbf{R}_T^{1/2} \in \mathbb{C}^{N_r \times L}$, where $\bar{\mathbf{G}}_k \in \mathbb{C}^{N_r \times L}$ denotes the channel between the last SIM layer and the receiver, distributed as $\mathcal{CN}(0, \beta \mathbf{I})$. The path-loss between the BS and user k is given by $\beta(d_k) = \beta(d_0) + 10b \log_{10}(d_k/d_0)$, where $\beta(d_0) = 20 \log_{10}(4\pi d_0/\lambda)$ is the free space path-loss at the reference distance d_0 , b is the path-loss exponent, and d_k is the distance between the BS and user k . Moreover, $\mathbf{R}_T \in \mathbb{C}^{L \times L}$ is the spatial correlation matrix of the SIM, defined as in [17, Eq. (14), (15)].

System Parameters: In the simulation setup, parameters are set as follows: $\lambda = 5$ cm (i.e., $f = 6$ GHz), $N_t = 16$, $N_r = 2$, $W = 100$ kHz, $b = 3.5$, $d_0 = 1$ m, $L = 4$, $K = 4$, $P_{\max} = 5$ W and $\sigma^2 = -110$ dB. Unless specified otherwise, the number of meta-elements per SIM layer, N , is 100. The BS antennas are placed in a planar array parallel to the xy -plane, with the midpoint at (30 m, 0, 0) and inter-antenna spacing of $\lambda/2$. SIM layers are also placed parallel to the xy -plane, with the midpoint of the l -th layer at (30 m, 0, $l\lambda/2$). Meta-elements, each with dimension $\lambda/2 \times \lambda/2$, are uniformly placed in a square grid on each SIM layer. Hence, any mutual coupling between different meta-elements can be neglected. Users' ULAs are parallel to the x -axis, with the midpoint of the k -th user's ULA at (x_k, y_k, z_k) . Users' coordinates are uniformly distributed such that $x_k \in [1.6 \text{ m}, 2 \text{ m}]$, $y_k \in [-20 \text{ m}, 20 \text{ m}]$, $z_k \in [80 \text{ m}, 120 \text{ m}]$. The circuit power per RF chain is $P_c = 30$ dBm, the basic power consumption at the BS is $P_0 = 40$ dBm [7], [26], and the power consumption per SIM meta-element is $P_s = 10$ dBm [27], [28]. Optimization parameters are set $\epsilon_D = 10^{-6}$ for DPC, and $\epsilon_{1,L} = \epsilon_{2,L} = 10^{-6}$ for LP. Gradient-based methods use an initial step size of 1000, $\rho = 1/2$ and $\delta = 10^{-3}$. Results are averaged over 200 independent channel realizations.

Initialization: For DPC the initial \mathbf{S}_k matrices are randomly generated Hermitian matrices satisfying (13b) with equality. For LP the initial \mathbf{X}_k are randomly generated matrices satisfying (42b) with equality. The initial elements of ϕ are randomly chosen from the unit circle.

The convergence of the proposed algorithms for different numbers of SIM layers is shown in Fig. 2. In general, we can see that the number of iterations required to converge increases with the number of SIM layers (i.e., meta-elements),

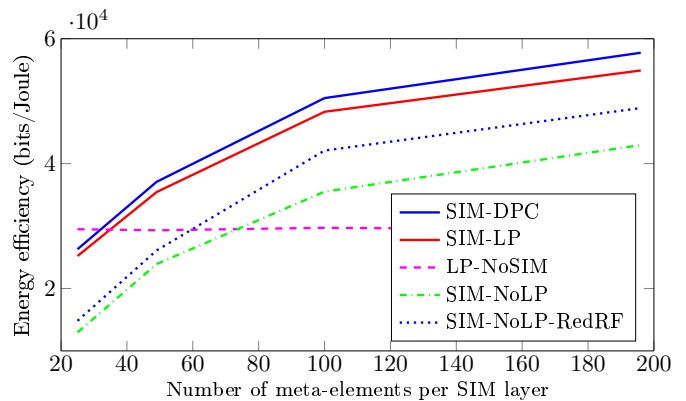


Fig. 3. EE versus number meta-elements per SIM layer.

consistent with previous observations in [18], where a layer-by-layer approach for SIM optimization was used. Notably, the gap in EE performance between SIM-DPC and SIM-LP remains small for any number of SIM layers, making *SIM-LP a practical and efficient solution for SIM-based systems*. Moreover, the EE is not monotonic with L . For SIM-DPC, the EE at convergence is almost the same for $L = 4$ and $L = 8$, while for SIM-LP, it is slightly higher when $L = 8$. This behavior results from the fact that the total power consumption scales linearly with the number of meta-elements, while the achievable sum-rate tends to be saturated [29, Fig. 4].

Fig. 3 shows the EE for different number meta-elements per SIM layer ($N = 25, 49, 100, 196$). The EE of both proposed and the non-precoding benchmark schemes (i.e., SIM-NoLP and SIM-NoLP-RedRF) increases with N but the increase rate gradually declines due to the logarithmic behavior of the achievable sum-rate at near-full transmit power. Among the non-precoding benchmarks, SIM-NoLP-RedRF achieves higher EE than SIM-NoLP due to reduced power consumption from inactive RF chains. Moreover, SIM-NoLP suffers from increased multi-stream interference as in this case each data stream is transmitted from two different transmit antennas without digital precoding, which potentially worsens as N increases, further enlarging the EE gap between these benchmarks. On the other hand, the saturation of the achievable sum-rate, and consequently the EE, with the further increase of the number of meta-elements results in almost the same enlargement of the EE for the two benchmark schemes. For a small N , LP-NoSIM achieves the largest EE, but is eventually inferior as other schemes benefit from an increased number of meta-elements. Finally, SIM-DPC achieves slightly higher EE than SIM-LP, with the gap increasing as N grows.

Fig. 4 plots the EE and the achievable sum-rate of the considered system versus the number of SIM layers, while keeping a total of 400 meta-elements. Importantly, we find that *SIM-LP is as good as SIM-DPC for both performance metrics*, regardless of the distribution of meta-elements on SIM layers, and *neither metric is monotonic with L* . Specifically, both increase from $L = 1$ to $L = 2$, which is apparently due to the enhanced beamforming capabilities offered by multi-layer structures. However, with L increases further, both performance metrics significantly decrease, potentially approaching LP-NoSIM. This occurs because fewer meta-

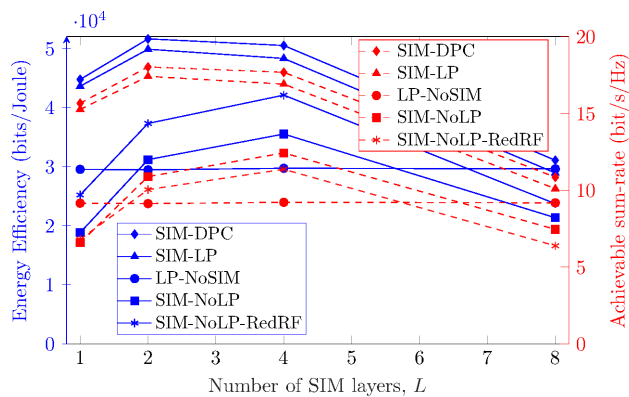


Fig. 4. EE (blue solid lines) and achievable sum-rate (red dashed lines) versus number SIM layer for the constant number of 400 meta-elements.

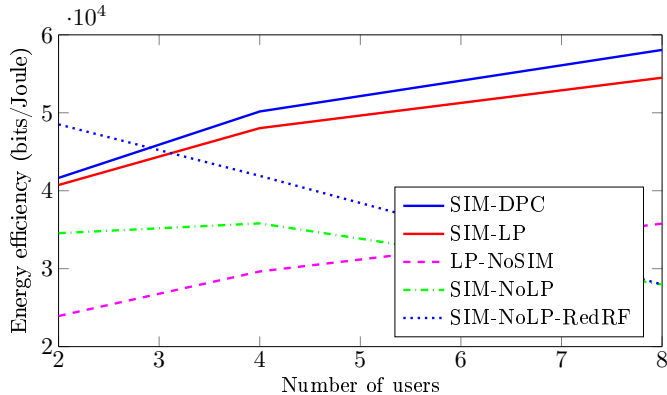


Fig. 5. The EE versus the number users.

elements per layer reduce the beamforming capability of each layer, while inter-layer propagation introduces additional path-loss as the number of SIM layers increases. A similar trend is observed in non-precoding benchmarks (i.e., SIM-NoLP and SIM-NoLP-RedRF), where the EE and the achievable sum-rate also decrease for $L > 4$. Among them, SIM-NoLP-RedRF achieves higher EE, despite a lower achievable sum-rate as it operates with fewer RF chains.

Fig. 5 demonstrates the EE for different number of users, K . For a small K , SIM-NoLP-RedRF provides the highest EE due to its reduced RF chain (and thus power) usage. However, as K increases, its EE declines since the number of RF chains becomes comparable to other schemes, and the lack of amplitude control of the transmitted signal limits its multi-user interference suppression capability [23]. On the other hand, the EE of SIM-NoLP shows a non-monotonic behavior with K . Specifically, its EE slightly improves from $K = 2$ to $K = 4$ due to the SIM being able to exploit multi-user diversity gains. However, when K further increases, the EE of both SIM-NoLP and SIM-NoLP-RedRF declines. The EE of the proposed SIM-based schemes and LP-NoSIM increase with K since digital precoding can effectively mitigate the multi-user interference, allowing them to exploit the multi-user diversity. Moreover, SIM-DPC achieves slightly higher EE than SIM-LP, and the gap widens as K increases. This observation further supports LP as an efficient, practical solution for SIM-based systems. Overall, we conclude that integrating SIM with digital precoding consistently yield the best EE, except for very small K .

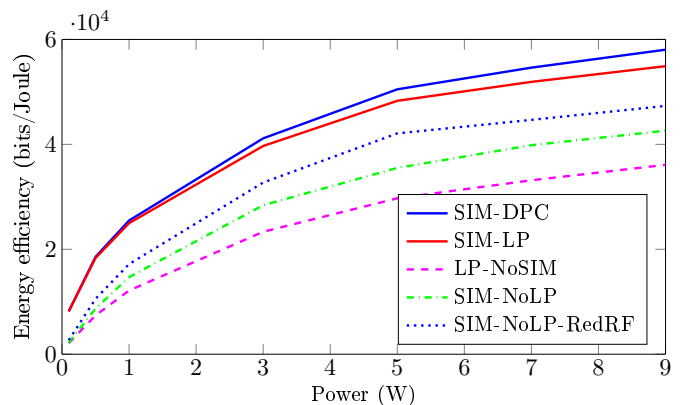


Fig. 6. EE versus the maximum transmit power.

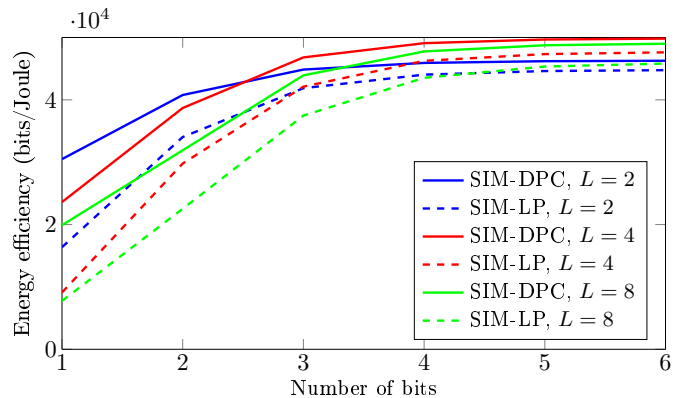


Fig. 7. EE for the case of discrete SIM phase shifts.

Next, Fig. 6 illustrates how the EE varies with the maximum transmit power. All schemes in consideration exhibit a logarithmic EE increase due to the logarithmic growth of the achievable rate. At low transmit power, the proposed schemes (i.e. SIM-DPC and SIM-LP) achieve the same EE, as do the benchmark schemes. As the transmit power increases, SIM-DPC consistently shows a more noticeable improvement in EE over all other schemes, which is attributed to the superior interference suppression capabilities of DPC. As expected, the proposed schemes outperform benchmark schemes, with, SIM-NoLP-RedRF obtaining the highest EE among them because of fewer RF chains being used. The difference in the EE between SIM-LP and other benchmark schemes increases with transmit power stabilizes at higher transmit power levels.

To assess the impact of realistic imperfections, Fig. 7 presents the EE of the proposed schemes for discrete SIM phase shifts. The EE generally deteriorates as the number of quantization bits decreases, especially for SIMs with a larger number of layers since the quantization errors are amplified. As a rule of thumb, at least 3 bits per meta-element are required for SIMs for a small L (e.g., 2 or 4) to maintain acceptable EE levels, while larger L requires finer resolution.

Finally, Fig. 8 shows the per-iteration computational complexity of the proposed optimization schemes versus the number of transmit antennas. The LP-NoSIM scheme achieves the lowest complexity compared to other schemes, as precoding without SIM involves much fewer elements than SIM meta-elements. Due to the same reason, the complexity of the

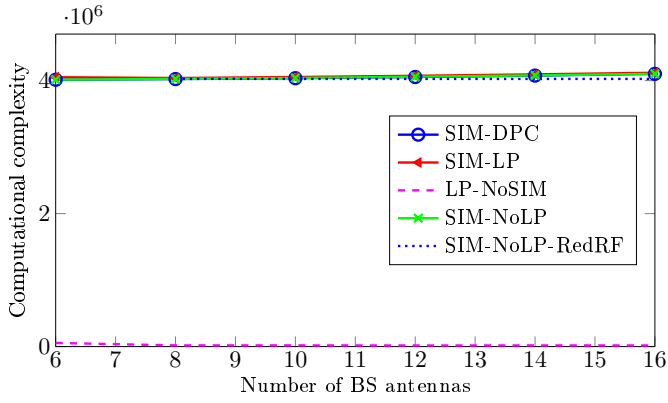


Fig. 8. Computational complexity versus the number transmit antennas.

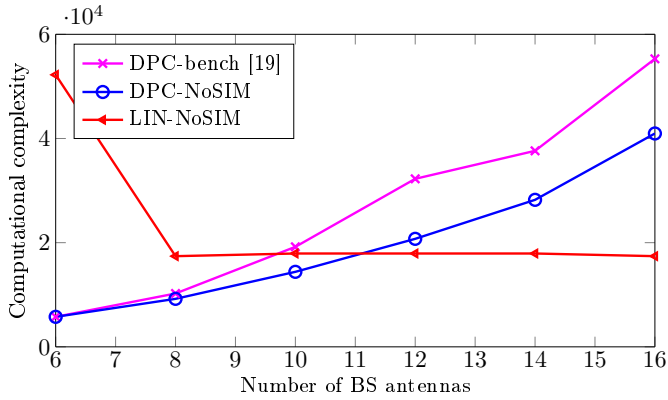


Fig. 9. Computational complexities of the proposed schemes with DPC and LP that are without the SIM, and the scheme from [19] versus the number transmit antennas.

benchmark schemes without precoding is very similar to that of the proposed schemes, and it is not even possible to observe any deference between DPC and LP.

To better highlight the difference between DPC and LP, we compare the computational complexities of their appropriate schemes without SIM (i.e., DPC-NoSIM and LP-NoSIM) in Fig. 9. As a benchmark, we consider the DPC-based scheme from [19], also without SIM, referred to as *DPC-bench*. Its complexity is $O(I_D K(N_t^2 N_r + N_t^3))$, where I_D is the required number of loops. It can be observed that LP-NoSIM has the highest complexity for $N_t = 6$ and $N_t < KN_r$. As N_t further increases, the complexities of DPC-NoSIM and DPC-bench become larger than that of LP-NoSIM. This is because the LP-NoSIM complexity remains approximately constant for $N_t \geq KN_r$, as indicated by (57). In addition, *DPC-bench* has a higher complexity than DPC-NoSIM, despite both achieving the same energy efficiency.

VIII. CONCLUSION, INSIGHTS, AND FUTURE WORK

In this paper, we studied the EE maximization in a SIM-aided broadcast system, considering both DPC and LP at the BS. For DPC, we exploited the well-known BC-MAC duality to reformulate the optimization problem and employed a SCA-based technique to derive a tight lower bound on the achievable sum-rate, which was then optimized using Dinkelbach's method. A similar approach was used to optimize precoders in the case of LP. The phase shifts of the SIM

meta-elements were optimized using a conventional projected gradient-based method due to its simplicity. Also, we conducted a computation complexity analysis of the proposed optimization algorithms and proved their convergence.

We carried out extensive numerical experiments and the simulation results have lead to the following insights which are useful for designing energy-efficient SIM-based systems:

- The proposed optimization algorithms significantly improve the EE for SIM-aided MIMO broadcast systems.
- DPC outperforms LP in terms of EE due to its superior interference cancellation, but the EE improvement remains marginal, *making LP a practical alternative with lower complexity*.
- SIM-based systems without digital precoding still suffer from higher multi-user interference, leading to lower EE.
- Increasing the number of meta-elements improves EE, but with diminishing returns due to increased power consumption and the logarithmic nature of the achievable sum-rate.
- Optimal meta-element distribution across layers is crucial; simply increasing the number of SIM layers can degrade performance due to inter-layer signal propagation loss.
- Discrete phase shift quantization negatively impacts EE, especially for systems with more SIM layers.
- In SIM-aided broadcast systems without digital precoding, optimal energy efficient transmission strategies typically involve a subset of active transmit antennas.

For future work, the above insights immediately motivate investigating the optimal distance between SIM layers to achieve the best EE performance. Another interesting topic is studying the performance of SIMs in a dynamic environment with user mobility, which would involve adapting the proposed optimization algorithms.

APPENDIX PROOF OF THEOREM 2

Differentiating $R_k(\phi)$ in (8) w.r.t. \mathbf{H}_k yields

$$dR_{L,k}(\phi) = d \ln |\mathbf{F}_{1,k}| - d \ln |\mathbf{F}_{2,k}| \quad (63)$$

where

$$d \ln |\mathbf{F}_{1,k}| = \text{Tr} \left(\hat{\mathbf{P}}_s \mathbf{H}_k^H \mathbf{F}_{1,k}^{-1} d\mathbf{H}_k + \mathbf{F}_{1,k}^{-1} \mathbf{H}_k \hat{\mathbf{P}}_s d\mathbf{H}_k^H \right) \quad (64)$$

$$d \ln |\mathbf{F}_{2,k}| = \text{Tr} \left(\hat{\mathbf{P}}_s \mathbf{H}_k^H \mathbf{F}_{2,k}^{-1} d\mathbf{H}_k + \mathbf{F}_{2,k}^{-1} \mathbf{H}_k \hat{\mathbf{P}}_k d\mathbf{H}_k^H \right). \quad (65)$$

Substituting (38) into the previous expressions, we obtain

$$d \ln |\mathbf{F}_{1,k}| = \text{Tr} \left(\mathbf{G}_1^H d\Phi^l + \mathbf{G}_1 d(\Phi^l)^H \right) \quad (66)$$

$$d \ln |\mathbf{F}_{2,k}| = \text{Tr} \left(\mathbf{G}_2^H d\Phi^l + \mathbf{G}_2 d(\Phi^l)^H \right) \quad (67)$$

where

$$\mathbf{G}_1 = \Theta^{l+1:L} \mathbf{G}_k^H \mathbf{F}_1^{-1} \mathbf{H}_k \hat{\mathbf{P}}_s \Theta^{1:l-1} \mathbf{W}_l^H \quad (68)$$

$$\mathbf{G}_2 = \Theta^{l+1:L} \mathbf{G}_k^H \mathbf{F}_2^{-1} \mathbf{H}_k \hat{\mathbf{P}}_k \Theta^{1:l-1} \mathbf{W}_l^H. \quad (69)$$

After a few simple mathematical steps, we get

$$\begin{aligned} \nabla_{\phi^l} R_{L,k}(\phi) = & \text{vec}_d \left(\Theta^{l+1:L} \mathbf{G}_k^H \mathbf{F}_{1,k}^{-1} \mathbf{H}_k \hat{\mathbf{P}}_s \Theta^{1:l-1} \mathbf{W}_l^H \right) \\ & - \text{vec}_d \left(\Theta^{l+1:L} \mathbf{G}_k^H \mathbf{F}_{2,k}^{-1} \mathbf{H}_k \hat{\mathbf{P}}_k \Theta^{1:l-1} \mathbf{W}_l^H \right). \end{aligned} \quad (70)$$

From this gradient expression for the achievable rate of user k , we can easily obtain the appropriate gradients for all other users. After summing all these gradient expressions, we obtain (55). This completes the proof.

REFERENCES

- [1] "Framework and overall objectives of the future development of int for 2030 and beyond," *International Telecommunication Union (ITU) Recommendation (ITU-R)*, 2023.
- [2] "Mobile data traffic outlook – Ericsson Mobility Report," 2024, [Accessed 05-07-2024]. [Online]. Available: <https://www.ericsson.com/en/reports-and-papers/mobility-report/dataforecasts/mobility-forecast>, 2024, Early Access.
- [3] M. Di Renzo *et al.*, "Smart radio environments empowered by reconfigurable intelligent surfaces: How it works, state of research, and the road ahead," *IEEE Journal on Selected Areas in Communications*, vol. 38, no. 11, pp. 2450–2525, 2020.
- [4] T. Gong *et al.*, "Holographic MIMO communications: Theoretical foundations, enabling technologies, and future directions," *IEEE Communications Surveys & Tutorials*, vol. 26, no. 1, pp. 196–257, 2024.
- [5] A. Zappone *et al.*, "Energy efficiency of holographic transceivers based on RIS," in *GLOBECOM 2022-2022 IEEE Global Communications Conference*. IEEE, 2022, pp. 4613–4618.
- [6] N. Shlezinger *et al.*, "Dynamic metasurface antennas for 6G extreme massive MIMO communications," *IEEE Wireless Communications*, vol. 28, no. 2, pp. 106–113, 2021.
- [7] L. You *et al.*, "Energy efficiency maximization of massive MIMO communications with dynamic metasurface antennas," *IEEE Transactions on Wireless Communications*, vol. 22, no. 1, pp. 393–407, 2022.
- [8] C. Liu *et al.*, "A programmable diffractive deep neural network based on a digital-coding metasurface array," *Nature Electronics*, vol. 5, no. 2, pp. 113–122, 2022.
- [9] J. An *et al.*, "Two-dimensional direction-of-arrival estimation using stacked intelligent metasurfaces," *arXiv preprint arXiv:2402.08224*, 2024.
- [10] Q.-U.-A. Nadeem *et al.*, "Hybrid digital-wave domain channel estimator for stacked intelligent metasurface enabled multi-user MISO systems," *arXiv preprint arXiv:2309.16204*, 2023.
- [11] Z. Wang *et al.*, "Multi-user ISAC through stacked intelligent metasurfaces: New algorithms and experiments," *arXiv preprint arXiv:2405.01104*, 2024.
- [12] N. U. Hassan *et al.*, "Efficient beamforming and radiation pattern control using stacked intelligent metasurfaces," *IEEE Open Journal of the Communications Society*, vol. 5, pp. 599–611, 2024.
- [13] J. An *et al.*, "Stacked intelligent metasurfaces for multiuser downlink beamforming in the wave domain," *arXiv preprint arXiv:2309.02687*, 2023.
- [14] A. Papazafeiropoulos *et al.*, "Achievable rate optimization for large stacked intelligent metasurfaces based on statistical CSI," *IEEE Wireless Communications Letters*, 2024, Early Access.
- [15] H. Liu *et al.*, "DRL-based orchestration of multi-user MISO systems with stacked intelligent metasurfaces," *arXiv preprint arXiv:2402.09006*, 2024.
- [16] Q. Li *et al.*, "Stacked intelligent metasurfaces for holographic MIMO aided cell-free networks," *IEEE Transactions on Communications*, 2024, Early Access.
- [17] J. An *et al.*, "Stacked intelligent metasurfaces for efficient holographic MIMO communications in 6G," *IEEE Journal on Selected Areas in Communications*, vol. 41, no. 8, pp. 2380–2396, 2023.
- [18] N. S. Perović and L.-N. Tran, "Mutual information optimization for SIM-based holographic MIMO systems," *arXiv preprint arXiv:2403.18307*, 2024.
- [19] J. Xu and L. Qiu, "Energy efficiency optimization for MIMO broadcast channels," *IEEE Transactions on Wireless Communications*, vol. 12, no. 2, pp. 690–701, 2013.
- [20] X. Lin *et al.*, "All-optical machine learning using diffractive deep neural networks," *Science*, vol. 361, no. 6406, pp. 1004–1008, 2018, Supplementary Material.
- [21] S. Vishwanath *et al.*, "Duality, achievable rates, and sum-rate capacity of gaussian MIMO broadcast channels," *IEEE Transactions on Information Theory*, vol. 49, no. 10, pp. 2658–2668, 2003.
- [22] H. H. M. Tam *et al.*, "Successive convex quadratic programming for quality-of-service management in full-duplex MU-MIMO multicell networks," *IEEE Transactions on Communications*, vol. 64, no. 6, pp. 2340–2353, 2016.
- [23] N. S. Perović *et al.*, "On the maximum achievable sum-rate of the risk-aided mimo broadcast channel," *IEEE Transactions on Signal Processing*, vol. 70, pp. 6316–6331, 2022.
- [24] X. Zhao *et al.*, "Rethinking WMMSE: Can its complexity scale linearly with the number of BS antennas?" *IEEE Transactions on Signal Processing*, vol. 71, pp. 433–446, 2023.
- [25] N. S. Perović *et al.*, "Achievable rate optimization for MIMO systems with reconfigurable intelligent surfaces," *IEEE Transactions on Wireless Communications*, vol. 20, no. 6, pp. 3865–3882, 2021.
- [26] S. He *et al.*, "Coordinated beamforming for energy efficient transmission in multicell multiuser systems," *IEEE Transactions on Communications*, vol. 61, no. 12, pp. 4961–4971, 2013.
- [27] J. Wang *et al.*, "Reconfigurable intelligent surface: Power consumption modeling and practical measurement validation," *IEEE Transactions on Communications*, 2024, Early Access.
- [28] C. Huang *et al.*, "Reconfigurable intelligent surfaces for energy efficiency in wireless communication," *IEEE Transactions on Wireless Communications*, vol. 18, no. 8, pp. 4157–4170, 2019.
- [29] A. Papazafeiropoulos *et al.*, "Achievable rate optimization for stacked intelligent metasurface-assisted holographic MIMO communications," *arXiv preprint arXiv:2402.16415*, 2024.